

# Minimum Mass and Optimal Complexity of Planar Tensegrity Bridges

Gerardo Carpentieri, Robert E. Skelton and Fernando Fraternali

Department of Civil Engineering, University of Salerno, Via Giovanni Paolo II, 132 – 84084 Fisciano (SA), Italy

Department of Structural Engineering, University of California San Diego, 9500 Gilman Dr., La Jolla, CA 92093, United States

Department of Civil Engineering, University of Salerno, Via Giovanni Paolo II, 132 – 84084 Fisciano (SA), Italy

(Submitted on 06/05/2015, Reception of revised paper 05/07/2015, Accepted on 08/04/2015)

**ABSTRACT:** This paper investigates the use of the most fundamental elements; cables for tension and bars for compression, in the search for the most efficient bridges. Stable arrangements of these elements are called tensegrity structures. We show herein the minimal mass arrangement of these basic elements to satisfy both yielding and buckling constraints. We show that the minimal mass solution for a simply-supported bridge subject to buckling constraints matches Michell's 1904 paper which treats the case of only yielding constraints, even though our boundary conditions differ. The necessary and sufficient condition is given for the minimal mass bridge to lie totally above (or below) deck. Furthermore this condition depends only on material properties. If one ignores joint mass, and considers only bridges above deck level, the optimal complexity (number of elements in the bridge) tends toward infinity (producing a material continuum). If joint mass is considered then the optimal complexity is finite. The optimal (minimal mass) bridge below deck has the smallest possible complexity (and therefore cheaper to build), and under reasonable material choices, yields the smallest mass bridge.

**Key Words:** tensegrity structures, form-finding, minimum mass, optimal complexity, deployable structures.

## 1. INTRODUCTION

Tensegrity is a word coined by Fuller in 1962 [1], as structures that are axially loaded prestressable structures with disjointed compressive members [2]. Skelton later enlarged the definition to include axially-loaded compressive members joined by ball joints and to include the presence of external forces in addition to prestress. This enlarged the design space for engineering purposes. Motivated by nature, where tensegrity concepts appear in every cell, in the molecular structure of the spider fiber, and in the arrangement of bones and tendons for control of locomotion in animals and humans [3], engineers

have only recently developed efficient analytical methods to exploit tensegrity concepts in engineering design. Previous attempts to judge the suitability of tensegrity for engineering purposes have simply evaluated the tensegrity produced as art-forms [4], but then judged them according to a different (engineering) criteria.

The tensegrity paradigm used for bridges in this paper allows the marriage of composite structures within the design. Our tensegrity approach creates a network of tension and compressive members distributed throughout the system at many different scales (using tensegrity fractals generates many

\*Corresponding author e-mail: gerardo\_carpentieri@msn.com

different scales). Furthermore, these tension and compression members can simultaneously serve multiple functions, as load-carrying members of the structure, and as sensing and actuating functions [5]. Moreover, the choice of materials for each member of the network can form a system with special electrical properties, special acoustic properties, special mechanical properties (stiffness, etc). The mathematical tools of this paper can be used therefore to design metamaterials with unusual and very special properties not available with normal design methods (cf., e.g., [5, 6]).

This paper focuses on bridge design for minimal mass. In particular, we focus our attention on *superstructure* and *substructure* bridges, that are well known in civil engineering, where they are often referred to as "tied arch" and "deck arch" bridges, respectively. An intermediate architecture is also known in the literature, the "through arch" bridges, referring to cases in which the deck runs half-way between the crown of an arch and the supporting piles. Remarkable examples of tied arch bridges are: the Lowry Avenue Bridge in Minneapolis, Minnesota over the Mississippi River; the Torikai big bridge over the Yodo river, Osaka, Japan; the GFRP Lleida Pedestrian Bridge. Furthermore, examples of deck arch bridges are given by: the Alexander Hamilton Bridge over the Harlem River in New York City; the Paderno bridge and Blera bridge in Italy [7]. Finally, benchmark examples of through arch bridges are: the Hell Gate Bridge, New York; the Bayonne Bridge, Staten Island, New York; the Tyne Bridge, Newcastle. We refer the reader to the interesting essay by Sergio Poretti and Tullia Iori on the history of structural engineering in Italy [7] for an exciting overview of arch bridges designed by worldwide known designers in Italy over the last 70 years (i.e. Maillart, Musumeci, Nervi, Morandi and Castiglano).

The present work aims at answering the long-standing question about the most convenient architecture of arch bridges, which is able to minimize the overall mass of the bridge structure and the deck. We show that shallow deck arch bridges offer minimal mass tensegrity architectures for simply supported bridges under uniformly distributed vertical loads. It is worth noting that tensegrity architectures provide minimal mass structural configurations for a variety of loading conditions, being able to resist to the applied loads without suffering mass-demanding bending stresses [8–11].

The subject of form-finding of tensegrity structures continues to be an active research area [12–17], due to the special ability of such structures to serve as

controllable systems (geometry, size, topology and prestress control), and also because the tensegrity architecture provides minimum mass structures for a variety of loading conditions, [8–11]. Other approaches to optimization can be found in [12, 17, 18]. These more general approaches can consider objective functions that include other criteria than minimal mass, but they do not yield analytical closed form expressions of the results. Such general methods also can lead to local minima rather than global answers.

Particularly interesting is the use of fractal geometry as a form-finding method for tensegrity structures, which is well described in [8–10, 18]. Such an optimization strategy exploits the use of fractal geometry to design tensegrity structures, through a finite or infinite number of self-similar subdivisions of basic modules. The strategy looks for the optimal number of self-similar iterations to achieve minimal mass or other design criteria. This number is called the optimal *complexity*, since this number fixes the total number of parts in the structure.

The self-similar tensegrity design presented in [8–10] is primarily focused on the generation of *minimum mass* structures, which are of great technical relevance when dealing with tensegrity bridge structures (refer, e.g., to [19]). The 'fractal' approach to tensegrity form-finding paves the way to an effective implementation of the tensegrity paradigm in *parametric architectural design* [13, 14, 20–22]. Discrete to continuum approaches to trusses and tensegrity structures are available in [23–26].

Designing tensegrity for engineering objectives has produced minimal mass solutions for five fundamental (but planar) problems in engineering mechanics. Minimal mass for tensile structures, (subject to a stiffness constraint) was motivated by the molecular structure of spider fiber, and may be found in [27]. Minimal mass for compressive loads may be found in [8]. Minimal mass for cantilevered bending loads may be found in [9]. Minimal mass for torsional loads may be found in [10]. Discussions of minimal mass solutions for distributed loads on simply-supported spans, where significant structure is not allowed below the roadway, may be found in [28].

This paper finds the minimum mass design of tensegrity structures carrying simply supported and distributed bending loads. In [28] numerical solutions were found for a specified topology, without any theoretical guarantees that those topologies produced minimal mass. This paper provides more fundamental proofs that provide necessary and sufficient conditions for minimal mass.

It is also worth noting that tensegrity structures can serve multiple functions. While a cable is a loadcarrying member of the structure, it might also serve as a sensor or actuator to measure or modify tension or length. Other advantages of tensegrity structures are related to the possibility to integrate control functions within the design of the structure. A grand design challenge in tensegrity engineering is to coordinate the structure and control designs to minimize the control energy and produce a structure of minimal mass. This would save resources (energy and mass) in two disciplines, and therefore "integrate" the disciplines [29].

The remainder of the paper is organized as follows. Section 2 provides some basic knowledges on the mode of failure of tensile and compressive members. Section 3 describes the topology of the tensegrity bridge under examination. For a simply-supported structure of the simplest complexity, Section 4 describes the minimal mass bridge when the admissible topology allows *substructure* and *superstructure* (that is, respectively, structure below and above the roadbed). Section 5 provides closed-form solutions to the minimal mass bridge designs (of complexity  $n = 1$ ) when only *substructure* or *superstructure* is allowed. Section 6 first defines deck mass and provides closed-form solutions to the minimal mass bridge designs (of complexity  $n, p = q = 1$ ) when only *substructure* or *superstructure* is allowed. This finalizes the proof that the minimal mass bridge is indeed the *substructure* bridge. Section 6 also adds joint mass and shows that the optimal complexity is finite. Conclusions are offered at the end.

## 2. PROPERTIES OF TENSILE AND COMPRESSIVE COMPONENTS OF THE TENSEGRITY STRUCTURE

The tensegrity structures in this paper will be composed of rigid compressive members called *bars*, and elastic tensile members called *cables*. We will assume that a tensile member obeys Hooke's law,

$$t_s = k(s - s_0), \quad (1)$$

where  $k$  is cable stiffness,  $t_s$  is tension in the cable,  $s$  is the length of the cable, and  $s_0 < s$  is the rest length of the cable. The tension members cannot support compressive loads. For our purposes, a compressive member is a solid cylinder, called a bar. All results herein are trivially modified to accommodate pipes, tubes of any material, but the concepts are more easily demonstrated and the presentation is simplified by using the solid bar in our derivations. The minimal

mass of a cable with yielding strength  $\sigma_s$  and mass density  $\rho_s$ , is

$$m_s = \frac{\rho_s}{\sigma_s} t_s s. \quad (2)$$

To avoid yielding, a bar of length  $b$ , yielding strength  $\sigma_b$ , mass density  $\rho_b$  with compression force  $f_b$ , has the minimal mass

$$m_{b,Y} = \frac{\rho_b}{\sigma_b} f_b b. \quad (3)$$

To avoid buckling, the minimal mass of a round bar of length  $b$ , modulus of elasticity  $E_b$ , and maximal force  $f_b$  is

$$m_{b,B} = 2\rho_b b^2 \sqrt{\frac{f_b}{\pi E_b}}. \quad (4)$$

The actual mode of failure (buckling or yielding) of a compressive member can be identified by using the following well-know facts that give the basis to a correct design of the bar radius  $r_b$ . Define  $r_Y$ , the bar radius that satisfies yielding constraints, and  $r_B$ , the radius that satisfies buckling constraints, by

$$r_Y = \sqrt{\frac{f_b}{\pi \sigma_b}}, \quad r_B = \sqrt[4]{\frac{4b^2 f_b}{\pi^3 E_b}}. \quad (5)$$

The following are well known facts:

**Lemma 2.1** *Designs subject to only yielding constraints (hence  $r_b = r_Y$ ) fail to identify the actual mode of failure (buckling) if  $r_Y < r_B$ , or equivalently if,*

$$\frac{f_b}{b^2} < \frac{4\sigma_b^2}{\pi E_b}. \quad (6)$$

**Lemma 2.2** *Designs subject to only yielding constraints ( $r_b = r_Y$ ) automatically also satisfy buckling constraints if  $r_Y > r_B$ , or equivalently if,*

$$\frac{f_b}{b^2} > \frac{4\sigma_b^2}{\pi E_b}. \quad (7)$$

**Lemma 2.3** *Designs subject to only buckling constraints ( $r_b = r_B$ ) fail to identify the actual mode of failure (yielding) if  $r_B < r_Y$ , or equivalently if,*

$$\frac{f_b}{b^2} > \frac{4\sigma_b^2}{\pi E_b}. \quad (8)$$

**Lemma 2.4** Designs subject to only buckling constraints ( $r_b = r_B$ ) automatically also satisfy yielding constraints if  $r_B > r_Y$ , or equivalently if,

$$\frac{f_b}{b^2} < \frac{4\sigma_b^2}{\pi E_b} \tag{9}$$

### 3. PLANAR TOPOLOGIES OF THE TENSEGRITY BRIDGES UNDER STUDY

The planar bridge topology is considered here to elucidate the fundamental properties that are important in the vertical plane. We use the following nomenclature, referring to Fig. 1:

- A *superstructure* bridge has no structure below the deck level.
- A *substructure* bridge has no structure above the deck level.
- A *nominal bridge* contains both *substructure* and *superstructure*.
- *Y* means the design was constrained against yielding for both cables and bars.
- *B* means the design was constrained against yielding for cables and buckling for bars.
- *n* means the number of self-similar iterations involved in the design ( $n = 1$  in Fig. 1, and  $n \geq 1$  in Fig. 2).
- *p* means the complexity of each iteration in the *substructure* ( $p = 1$  in Fig. 1c, and  $p \geq 1$  in Fig. 2).
- *q* means the complexity of each iteration in the *superstructure* ( $q = 1$  in Fig. 1b, and  $q \geq 1$  in Fig. 2).
- $\alpha$  is the aspect angle of the *superstructure* measured from the horizontal.
- $\beta$  is the aspect angle of the *substructure* measured from the horizontal.

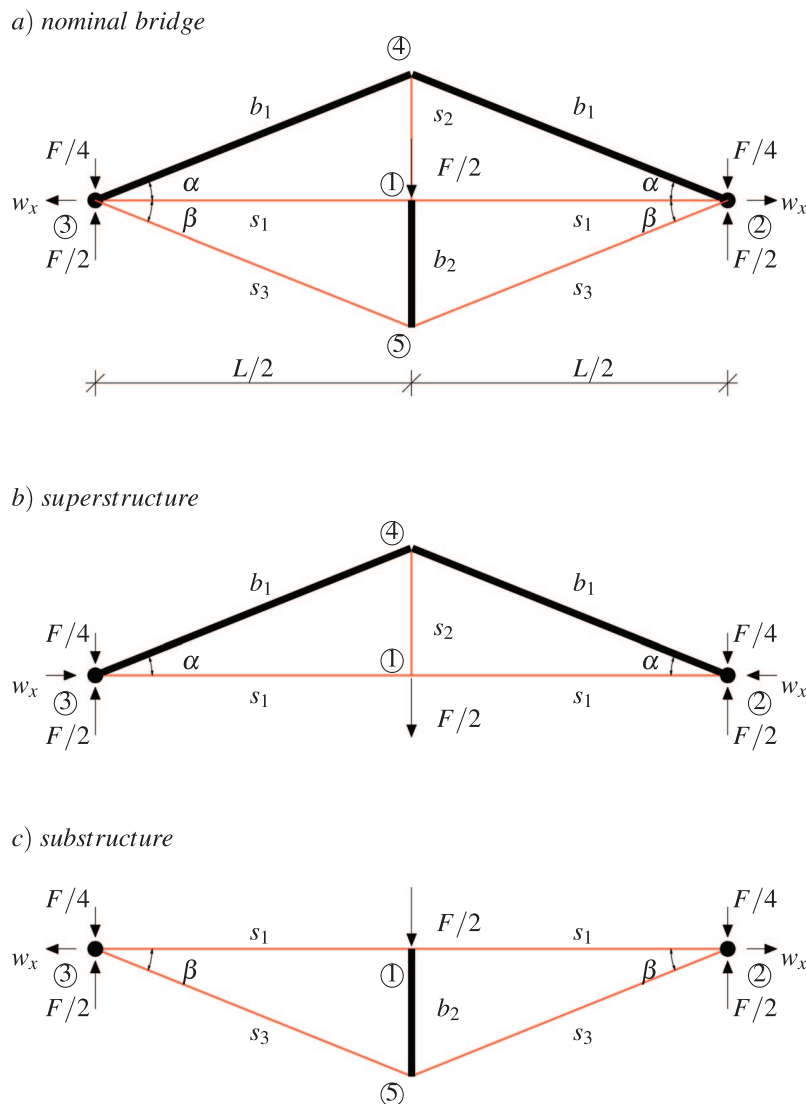


Figure 1. Basic modules of the tensegrity bridge with: a) *nominal bridge*:  $n = q = p = 1$ ; b) *superstructure*:  $n = q = 1$ ; c) *substructure*:  $n = p = 1$ . Compressive members (bars) are heavy black lines, tensile members (cables) are thin red lines.

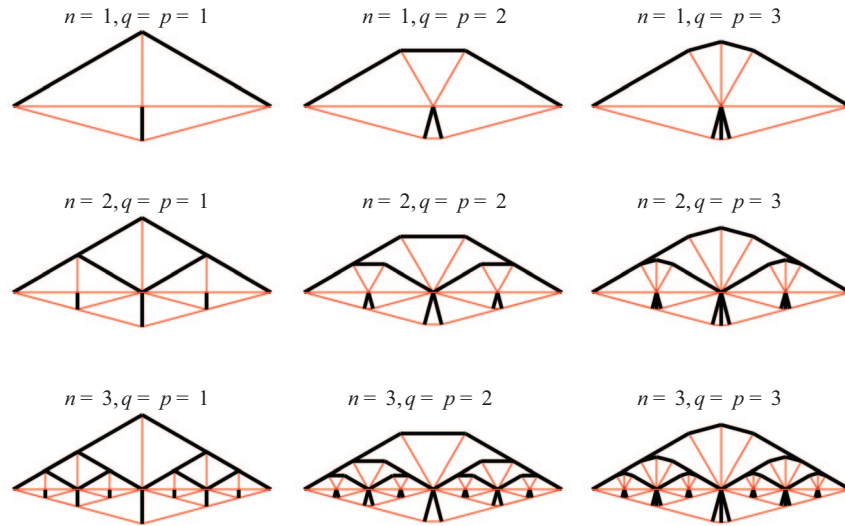


Figure 2. Typical topologies of the *nominal* bridges for different values of the complexity parameters  $n$  (increasing downward) and  $q, p$  (increasing rightward).

For a tensegrity bridge with generic complexities  $n$ ,  $p$  and  $q$  (see Fig. 2), the total number of nodes  $n_n$  of each topology is given by:

$$n_n = (p+q)(2^n - 1) + 2^n + 1. \quad (10)$$

For the *substructure* bridge (that is  $q = 0$ ), the number of bars  $n_b$  and the number of cables  $n_s$  are:

$$n_b = p(2^n - 1), \quad n_s = (p+1)(2^n - 1) + 2^n. \quad (11)$$

For the *superstructure* bridge (that is  $p = 0$ ), the number of bars  $n_b$  and the number of cables  $n_s$  are:

$$n_b = (q+1)(2^n - 1), \quad n_s = q(2^n - 1) + 2^n. \quad (12)$$

For the *nominal* bridge, the number of bars  $n_b$  and the number of cables  $n_s$  are:

$$n_b = (p+q+1)(2^n - 1), \quad n_s = (p+q+1)(2^n - 1) + 2^n. \quad (13)$$

We define the *superstructure* bridge of complexity  $(n, p = 0, q)$  by Fig. 2 where the *substructure* below is deleted. We define the *substructure* bridge of complexity  $(n, p, q = 0)$  by Fig. 2 where the *superstructure* above is deleted.

#### 4. ANALYSIS OF THE BASIC MODULES ( $n = 1, p = 1$ OR $0, q = 1$ OR $0$ )

We first will examine the simplest of bridge concepts, as in Fig. 1. Consider, first, the *nominal* bridge, subject to yielding constraints, with complexity  $(n, p, q) = (1, 1, 1)$ . This configuration, described by Fig. 1a, is composed of 5 cables and 3 bars. Let the bottom end of each compressive member above the deck be

constrained by a hinge boundary condition, so as to allow rotation but not translation. Define  $F$  as the total applied load, and  $L$  as the span. All cables use the same material, and all bars use the same material. It will be convenient to define the following constants:

$$\rho = \frac{\rho_b / \sigma_b}{\rho_s / \sigma_s}, \quad (14)$$

$$\eta = \frac{\rho_b L}{(\rho_s / \sigma_s) \sqrt{\pi E_b F}}. \quad (15)$$

Define a normalization of the system mass  $m$  by the dimensionless quantity  $\mu$ :

$$\mu = \frac{m}{(\rho_s / \sigma_s) FL}, \quad (16)$$

where the mass  $m$  at the yielding condition is:

$$m = \frac{\rho_b}{\sigma_b} \sum f_i b_i + \frac{\rho_s}{\sigma_s} \sum t_i s_i, \quad (17)$$

where  $(b_i, s_i)$  is respectively the length of the  $i^{th}$  bar or cable, and respectively  $(f_i, t_i)$  is the force in the  $i^{th}$  bar or cable.

The mass of the *nominal* bridge will be minimized over the choice of angles  $\alpha$  and  $\beta$ . The lengths of the members are:

$$s_1 = \frac{L}{2}, \quad s_2 = \frac{L}{2} \tan \alpha, \quad s_3 = \frac{L}{2 \cos \beta} = \frac{L}{2} \sqrt{1 + \tan^2 \beta},$$

$$b_1 = \frac{L}{2 \cos \alpha} = \frac{L}{2} \sqrt{1 + \tan^2 \alpha}, \quad b_2 = \frac{L}{2} \tan \beta. \quad (18)$$

The equilibrium equations at each node are:

$$\begin{aligned} t_1 + t_3 \cos \beta &= w_x + f_1 \cos \alpha, \\ \frac{F}{4} &= f_1 \sin \alpha + t_3 \sin \beta, \\ t_2 &= 2f_1 \sin \alpha, \\ f_2 &= 2t_3 \sin \beta, \\ \frac{F}{2} &= t_2 + f_2. \end{aligned} \tag{19}$$

This system of equations can be solved, choosing  $t_1$  and  $t_3$  as free independent parameters:

$$\begin{aligned} \frac{f_1}{F} &= \frac{\sqrt{1 + \tan^2 \alpha}}{4 \tan \alpha} \left( 1 - \frac{t_3}{F} \frac{4 \tan \beta}{\sqrt{1 + \tan^2 \beta}} \right), \\ \frac{f_2}{F} &= \frac{t_3}{F} \frac{2 \tan \beta}{\sqrt{1 + \tan^2 \beta}}, \\ \frac{t_2}{F} &= \frac{1}{2} - \frac{t_3}{F} \frac{2 \tan \beta}{\sqrt{1 + \tan^2 \beta}}, \\ \frac{w_x}{F} &= \frac{t_1}{F} + \frac{t_3}{F} \frac{\tan \alpha + \tan \beta}{\tan \alpha \sqrt{1 + \tan^2 \beta}} - \frac{1}{4 \tan \alpha}. \end{aligned} \tag{20}$$

#### 4.1. Nominal bridges under yielding constraints

The nominal bridge of complexity  $(n, p, q) = (1, 1, 1)$  subject to yielding constraints is optimized in the following theorem.

**Theorem 4.1** *Given the nominal bridge with complexity  $(n, p, q) = (1, 1, 1)$  (described in Fig. 1a), with attendant data (18), the minimal mass can be expressed in terms of independent variables  $t_1$  and  $t_3$ :*

$$\mu_Y(t_1, t_3) = \frac{t_1}{F} + \frac{t_3}{F} c_3(\alpha, \beta, \rho) + \frac{b_\alpha}{4}, \tag{21}$$

where:

$$\begin{aligned} c_3(\alpha, \beta, \rho) &= \frac{(1 + \rho) \tan^2 \beta - b_\alpha \tan \beta + 1}{\sqrt{1 + \tan^2 \beta}}, \\ b_\alpha &= \frac{\rho + (1 + \rho) \tan^2 \alpha}{\tan \alpha}. \end{aligned} \tag{22}$$

An alternate expression for the mass can be written by substituting the relation between  $t_2$  and  $t_3$  from (27), to get an equivalent expression  $\mu_Y(t_1, t_2) = \mu_Y(t_1, t_3)$ , where:

$$\frac{t_3}{F} = \frac{\sqrt{1 + \tan^2 \beta} (1 - 2t_2/F)}{4 \tan \beta}, \tag{23}$$

$$\mu_Y(t_1, t_2) = \frac{t_1}{F} + \frac{t_2}{F} c_2(\alpha, \beta, \rho) + \frac{(1 + \rho) \tan^2 \beta + 1}{4 \tan \beta}, \tag{24}$$

$$\begin{aligned} c_2(\alpha, \beta, \rho) &= -c_3 \frac{\sqrt{1 + \tan^2 \beta}}{2 \tan \beta} \\ &= -\frac{(1 + \rho) \tan^2 \beta - b_\alpha \tan \beta + 1}{2 \tan \beta}. \end{aligned} \tag{25}$$

Hence it follows that the minimal mass solution requires  $t_3 > 0$  if and only if  $c_3 < 0$  (equivalently  $c_2 > 0$ ). Note also that  $c_3 < 0$  if and only if:

$$\frac{1 + (1 + \rho) \tan^2 \beta}{\tan \beta} < \frac{\rho + (1 + \rho) \tan^2 \alpha}{\tan \alpha}. \tag{26}$$

Conversely, minimal mass requires  $t_3 = 0$  if  $c_3 > 0$  (equivalently  $c_2 < 0$ ). This event occurs if and only if:

$$\frac{1 + (1 + \rho) \tan^2 \beta}{\tan \beta} > \frac{\rho + (1 + \rho) \tan^2 \alpha}{\tan \alpha}. \tag{27}$$

Finally,  $c_3 = 0$  (and also  $c_2 = 0$ ) if and only if:

$$\frac{1 + (1 + \rho) \tan^2 \beta}{\tan \beta} = \frac{\rho + (1 + \rho) \tan^2 \alpha}{\tan \alpha}. \tag{28}$$

Note also that the requirement that  $t_2$  and  $t_3$  both be non-negative values limits the feasible range of  $t_3$  such that:

$$0 \leq t_3 \leq \frac{F \sqrt{1 + \tan^2 \beta}}{4 \tan \beta}. \tag{29}$$

Given the relation between  $t_2$  and  $t_3$  in (23) we have the corresponding feasible range for  $t_2$ :

$$0 \leq t_2 \leq \frac{F}{2}. \tag{30}$$

The proof of the theorem follows the mass calculation in (16), (17) after substituting the equilibrium forces given by (20).

**Corollary 4.1** *Consider a superstructure bridge with complexity  $(n, p, q) = (1, 0, 1)$  (topology is defined by Fig. 1b). The minimal mass  $\mu_Y$  requires the following aspect angle:*

$$\alpha_Y^* = \arctan \left( \sqrt{\frac{\rho}{1 + \rho}} \right), \tag{31}$$

which corresponds to the following dimensionless minimal mass:

$$\mu_Y^* = \frac{1}{2} \sqrt{\rho(1+\rho)}. \quad (32)$$

From (32) and (21) notice that  $t_1 = t_3 = 0$  in the minimal mass *substructure*. As a practical matter the cable 1, would not actually be eliminated but it would be prestressed with a small tension to stabilize the midpoint in presence of horizontal dynamic forces.

Refer to [30] for an extended proof of the above and following corollaries of this section.

**Corollary 4.2** Consider a substructure bridge, with complexity  $(n, p, q) = (1, 1, 0)$  (topology is defined by Fig. 1c). The minimal mass design under only yielding constraints is given by the following aspect angle:

$$\beta_Y^* = \arctan\left(\frac{1}{\sqrt{1+\rho}}\right), \quad (33)$$

which corresponds to the following dimensionless minimal mass:

$$\mu_Y^* = \frac{\sqrt{1+\rho}}{2}. \quad (34)$$

Figure 3 plots the mass versus the angles  $\beta$  and  $\alpha$ , yielding the minimum at the values given by (33) and (31). All designs in this section assume failure by yielding. One must check that yielding is indeed the mode of failure.

**Corollary 4.3** For the designs in this section, yielding is indeed the mode of failure if the following inequalities hold:

$$\frac{F}{L^2} > \frac{1}{2(1+\rho)} \left( \frac{4\sigma_b^2}{\pi E_b} \right), \quad \text{if: } 0 < \rho \leq \frac{1}{4}(\sqrt{3}-1), \quad (35)$$

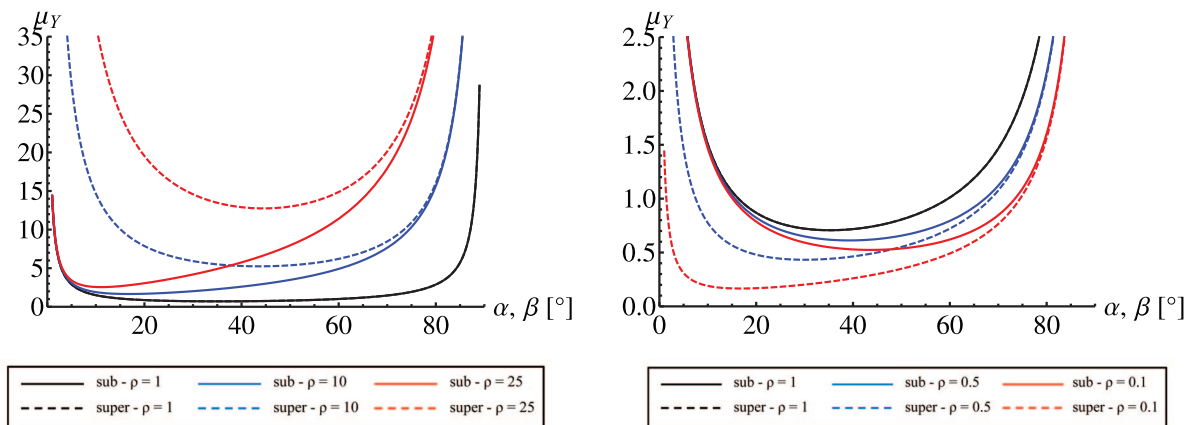


Figure 3. Dimensionless masses of the *substructure* (continuous curves) and *superstructure* (dashed curves) for different values of the aspect angles (respectively  $\beta$  or  $\alpha$ ) and for values of the coefficient  $\rho > 1$  (left) and  $\rho < 1$  (right) under yielding constraints.

$$\frac{F}{L^2} > \frac{\sqrt{\rho(1+2\rho)}}{1+\rho} \left( \frac{4\sigma_b^2}{\pi E_b} \right), \quad \text{if: } \rho > \frac{1}{4}(\sqrt{3}-1), \quad (36)$$

In addition, if  $0 < \rho \leq \frac{1}{4}(\sqrt{3}-1)$  and (35) holds or if

$\frac{1}{4}(\sqrt{3}-1) < \rho < 1$  and (36) holds, then the minimal

mass of a superstructure bridge is less than the minimal mass of a substructure bridge. (In this event, the minimal mass bridge is superstructure only). If  $\rho = 1$  and (36) also holds, then the minimal mass of the substructure bridge is equal to the minimal mass of the superstructure bridge. If  $\rho > 1$  and (36) also hold, then the minimal mass of the substructure bridge is less than the minimal mass of the superstructure bridge. If  $\rho > 1$  and (36) also hold, then the minimal mass of the substructure bridge is less than the minimal mass of the superstructure bridge (The minimal mass bridge is substructure only).

As a practical matter,  $\rho$  is almost always greater than 1, since compressive members tend to have a mass density over yielding strength ratio greater than cables (i.e.  $(\rho_b/\sigma_b) > (\rho_s/\sigma_s)$ ).

Thus far the conclusion is that if  $\rho > \frac{1}{4}(\sqrt{3}-1)$  then the bridge in Fig. 1a at its minimal mass configuration becomes the configuration of *substructure* in Fig. 1c, if the bridge design is constrained against yielding. Furthermore, such a design will not buckle. Note that this design produced a topology constrained against yielding, and a design constrained against buckling might produce a different topology. Now let's consider this possibility.

4.2. Nominal bridges under buckling constraints

This section repeats all the designs of the previous section (for the three structures of Fig. 1) with the added constraint that the bars cannot buckle.

**Theorem 4.2** Consider a nominal bridge of complexity  $(n, p, q) = (1, 1, 1)$ . The minimal mass (the cable mass required at the yielding conditions plus the bar mass required at the bar buckling conditions), is, in terms of  $t_1$  and  $t_3$ :

$$\begin{aligned} \mu_B(t_1, t_3) = & \frac{t_1}{F} + \frac{t_3}{F} \frac{\tan^2 \beta - \tan \alpha \tan \beta + 1}{\sqrt{1 + \tan^2 \beta}} + \frac{\tan \alpha}{4} \\ & + \eta \left[ \frac{(1 + \tan^2 \alpha)^{5/4}}{2\sqrt{\tan \alpha}} \left( 1 - \frac{t_3}{F} \frac{4 \tan \beta}{\sqrt{1 + \tan^2 \beta}} \right)^{1/2} \right. \\ & \left. + \frac{\tan^2 \beta}{\sqrt{2}} \sqrt{\frac{t_3}{F} \frac{\tan \beta}{(1 + \tan^2 \beta)^{1/2}}} \right], \end{aligned} \tag{37}$$

or, equivalently, in terms of  $t_1$  and  $t_2$ :

$$\begin{aligned} \mu_B(t_1, t_2) = & \frac{t_1}{F} + \frac{t_2}{F} \left[ \frac{\tan \alpha}{2} - \frac{(1 + \tan^2 \beta)}{2 \tan \beta} \right] + \frac{(1 + \tan^2 \beta)}{4 \tan \beta} \\ & + \eta \left[ (1 + \tan^2 \alpha)^{5/4} \sqrt{\frac{t_2}{2F \tan \alpha}} + \frac{\tan^2 \beta}{2} \sqrt{\frac{1}{2} - \frac{t_2}{F}} \right]. \end{aligned} \tag{38}$$

Refer to [30] for an extended proof of the above theorem.

The value of  $\beta = 4.25 \text{ deg}$  minimizes the mass (38) if the material choice is steel ( $\rho = 7862 \text{ kg/m}^3$ ;  $\sigma = 6.9 \times 10^8 \text{ N/m}^2$ ;  $E = 2.06 \times 10^{11} \text{ N/m}^2$ ). It will become clear that the minimal mass solution of the minimal bridge  $\mu_B$ , constrained against buckling, will reduce to only a *substructure*. It is straightforward to show that the mass of the bars is much greater than the mass of the cables under the usual condition:

$$\eta \gg \frac{\tan^2 \alpha}{2(1 + \tan^2 \alpha)^{5/4}}. \tag{39}$$

To prepare for those insights, now consider the individual solutions for designs constrained to be only *superstructure* or only *substructure* in configuration.

**Corollary 4.4** Consider a superstructure bridge of complexity  $(n, p, q) = (1, 0, 1)$ , (Fig. 1b). Suppose (39) holds. The minimal mass design under yielding and buckling constraints is given by the following aspect angle:

$$\bar{\alpha}_B^* = \arctan\left(\frac{1}{2}\right), \tag{40}$$

which corresponds to the following dimensionless minimal mass:

$$\bar{\mu}_B^* = \frac{1}{8}(1 + 5^{5/4})\eta. \tag{41}$$

Refer to [30] for an extended proof of the above and following corollaries of this section.

It is straightforward to show that the second variation of  $\mu_B(\alpha)$  with respect to  $\alpha$  is always positive, indicating that there is only one minimum described by (40).

**Corollary 4.5** Consider a substructure bridge, with complexity  $(n, p, q) = (1, 1, 0)$  (Fig. 1c). The minimal mass design under yielding constraints and buckling constraints is given by the following aspect angle:

$$\beta_B^* = \arctan\left[\frac{1}{6\eta} \left( \frac{1}{2^{1/3}\epsilon} + \frac{\epsilon}{2^{2/3}} - \frac{1}{\sqrt{2}} \right)\right], \tag{42}$$

which corresponds to the following dimensionless minimal mass:

$$\mu_B^* = \frac{1 + \tan^2 \beta_B^*}{4 \tan \beta_B^*} + \frac{\eta}{2\sqrt{2}} \tan^2 \beta_B^*, \tag{43}$$

where:

$$\epsilon = \left[ 108\sqrt{2}\eta^2 + \sqrt{2332\eta^4 - 432\eta^2 - \sqrt{2}} \right]^{1/3}. \tag{44}$$

It is straightforward to show that the second variation of  $\mu_B(\beta)$  with respect to  $\beta$  is always positive, indicating a unique global optimal value of (42). Figure 4 plots the mass versus the angle  $\beta$  and  $\alpha$ , yielding the minimum at the values given by (40) and (42).

We must verify if buckling is indeed the mode of failure in the designs of this section.

**Corollary 4.6** Suppose buckling constraints are considered in both superstructure and substructure bridge designs. Then buckling is indeed the mode of failure if the following inequalities hold:

$$\frac{F}{L^2} < \tan \alpha \sqrt{1 + \tan^2 \alpha} \left( \frac{4\sigma_b^2}{\pi E_b} \right), \quad \text{if: } \bar{\eta}_{\alpha\beta} < 1, \tag{45}$$

$$\frac{F}{L^2} < \frac{\tan^2 \beta}{2} \left( \frac{4\sigma_b^2}{\pi E_b} \right), \quad \text{if: } \bar{\eta}_{\alpha\beta} > 1, \tag{46}$$

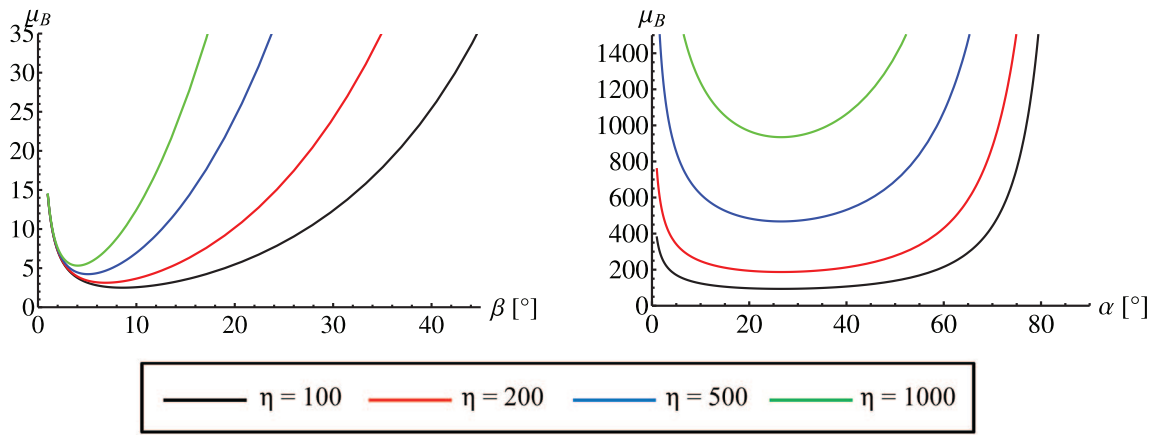


Figure 4. Dimensionless masses of the *substructure* (left) and *superstructure* (right) under buckling constraints for different values of the aspect angles (respectively  $\beta$  or  $\alpha$ ) and different values of the parameter  $\eta$ .

where

$$\bar{\eta}_{\alpha\beta} = \frac{2 \tan \alpha \sqrt{1 + \tan^2 \alpha}}{\tan^2 \beta} \quad (47)$$

In addition, if the following inequality holds:

$$\eta > \eta_{\alpha\beta} = \frac{-(\tan \alpha)^{(3/2)} \tan \beta + (1 + \tan^2 \beta) \sqrt{\tan \alpha}}{2(1 + \tan^2 \beta)^{(5/4)} \tan \beta - \sqrt{2} \tan^3 \beta \sqrt{\tan \alpha}}, \quad (48)$$

then the minimal mass of the substructure bridge is less than the minimal mass of the superstructure bridge. (The minimal mass of the nominal bridge reduces to substructure only. If  $\eta = \eta_{\alpha\beta}$ , (45) or (46) hold, then the minimal mass of the substructure is equal to the minimal mass of the superstructure. (The minimal mass of the nominal bridge reduces to either superstructure or substructure only). If  $\eta < \eta_{\alpha\beta}$ , and (45) or (46) hold, then the minimal mass of the superstructure is less than the minimal mass of the substructure. (The minimal mass bridge is superstructure only).

### 5. MASS OF BRIDGES OF COMPLEXITY $(n, p, q) = (1, p, q)$ , UNDER YIELDING AND BUCKLING CONSTRAINTS

Now we consider more complex structures by increasing  $p, q$ . This section finds the minimal mass of *substructure*, and *superstructure* bridges with complexity  $(n, p, q) = (1, p, q)$ , for any  $p$  and  $q$  greater than 1.

#### 5.1. Substructure bridge with complexity $(n, p, q) = (1, p > 1, 0)$

Refer to Fig. 5 for the notation. The angle between the bars is:

$$\gamma = \frac{2\beta}{p-1}. \quad (49)$$

The lengths of the bars and cables are:

$$s_0 = \frac{L}{2}, \quad s_1 = \frac{L}{2} \cos \beta, \quad (50)$$

$$s = L \sin \beta \sin \left( \frac{\beta}{p-1} \right), \quad b_1 = b_2 = \frac{L}{2} \sin \beta.$$

From the equilibrium equations, we obtain the following relations for the forces:

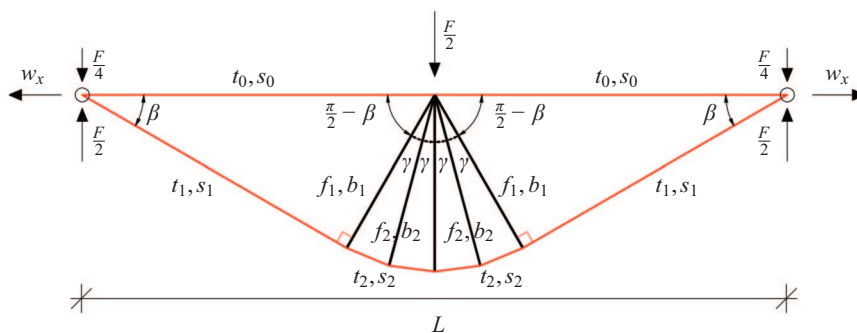


Figure 5. Notations for forces and lengths of bars and cables for a *substructure* with complexity  $n = 1$  and  $p > 1$ .

$$f_1 = \frac{F}{4 \left[ \cos \beta + \sin \left( \frac{\beta(p-2)}{p-1} \right) / \sin \left( \frac{\beta}{p-1} \right) \right]}, \quad f_2 = 2f_1, \quad (51)$$

$$t_2 = \frac{f_2}{2 \sin \left( \frac{\beta}{p-1} \right)}, \quad t_1 = t_2 \cos \left( \frac{\beta}{p-1} \right). \quad (52)$$

**Theorem 5.1** Consider a substructure bridge with topology described by (50), with complexity  $(n, p, q) = (1, p, 0)$  (Fig. 5). At the yielding condition the dimensionless total mass is:

$$\mu_Y(\beta, p) = \frac{t_0}{F} + \frac{1}{4} \left[ \frac{(p-1) \sin \beta \sin \left( \frac{\beta}{p-1} \right) + \cos \beta \cos \left( \frac{\beta}{p-1} \right)}{\cos \beta \sin \left( \frac{\beta}{p-1} \right) + \sin \left( \frac{\beta(p-2)}{p-1} \right)} \right] + \rho \frac{(p-1) \sin \beta}{4 \left[ \cos \beta + \sin \left( \frac{\beta(p-2)}{p-1} \right) / \sin \left( \frac{\beta}{p-1} \right) \right]}. \quad (53)$$

Refer to [30] for an extended proof of the above theorem and following theorems of this section.

**Corollary 5.1** The minimal mass in (53) is achieved at infinite complexity  $p \rightarrow \infty$  and  $t_0 = 0$ . The minimal mass at yielding for a substructure bridge is:

$$\mu_Y^*(\beta_Y^*, p^*) = \frac{1}{4} \left[ \sqrt{\rho} + (1 + \rho) \arctan \frac{1}{\sqrt{\rho}} \right], \quad (54)$$

where  $p^* \rightarrow \infty$  and the optimal angle  $\beta_Y^*$  is:

$$\beta_Y^* = \arctan \left( \frac{1}{\sqrt{\rho}} \right). \quad (55)$$

**Proof 5.1** Substitute  $p \rightarrow \infty$  into Eq. (53) to obtain:

$$\mu_Y^*(\beta, \rho^* \rightarrow \infty) = \frac{\beta}{4} (1 + \rho) + \frac{1}{4 \tan \beta}. \quad (56)$$

The value of  $\beta$  that minimizes (56) is (55). Figure 6 shows how mass (53) varies with  $p$  and  $\beta$ . The optimal  $p^*$  is deduced from the plot of Fig. 6 and the optimal angle is computed analytically in Eq. (55).

**Theorem 5.2** Consider a substructure bridge with topology defined by (50), with complexity  $(n, p, q) = (1, p, 0)$ , See Fig. 5. At the buckling condition the dimensionless total mass is minimized at  $p = 2$  and  $t_0 = 0$ , where:

$$\mu_B(\beta, p = 2) = \frac{1 + \tan^2 \beta}{4 \tan \beta} + \frac{\eta}{2} \frac{\tan^2 \beta}{(1 + \tan^2 \beta)^{3/4}}. \quad (57)$$

**Corollary 5.2** The minimal mass substructure is achieved for  $p = 1$ .

**Proof 5.2** The mass of a substructure with topology of  $n = 1$  defined by (50), for a general  $p > 1$  is:

$$\mu_B(\beta, p) = \frac{t_0}{F} + \frac{1}{4} \left[ \frac{(p-1) \sin \beta \sin \left( \frac{\beta}{p-1} \right) + \cos \beta \cos \left( \frac{\beta}{p-1} \right)}{\cos \beta \sin \left( \frac{\beta}{p-1} \right) + \sin \left( \frac{\beta(p-2)}{p-1} \right)} \right] + \frac{\eta}{2\sqrt{2}} \frac{(p-2 + \sqrt{2}) \sin^2 \beta}{\sqrt{\cos \beta + \sin \left( \frac{\beta(p-2)}{p-1} \right) / \sin \left( \frac{\beta}{p-1} \right)}}. \quad (58)$$

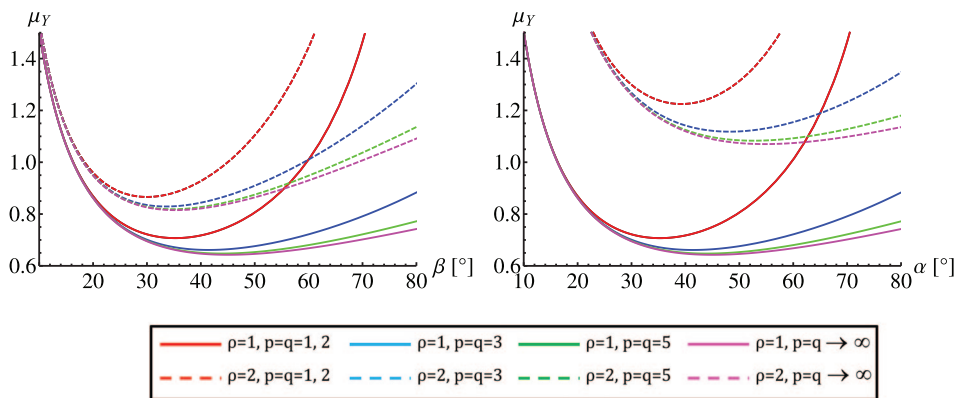


Figure 6. Mass curves under yielding constraints of substructures (left) and superstructures (right) vs. aspect angle  $\beta$  (left) and  $\alpha$  (right) for different complexity  $p$  (left) and  $q$  (right), ( $F = 1 \text{ N}, L = 1 \text{ m}$ ).

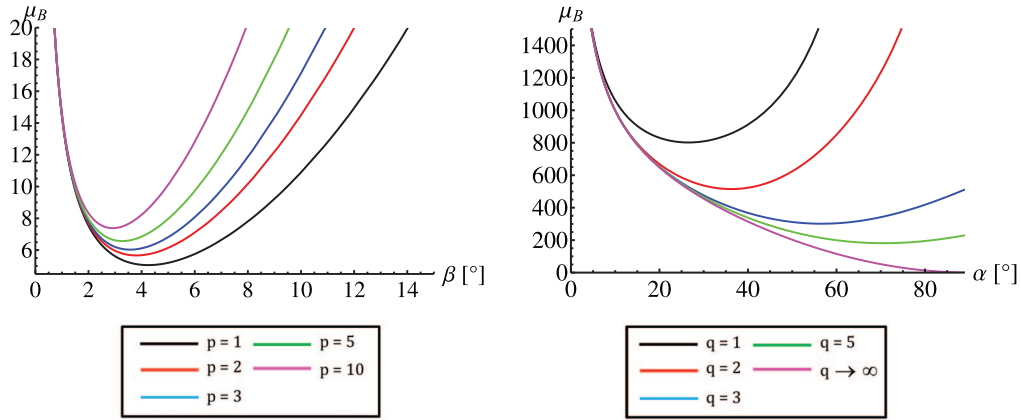


Figure 7. Mass curves under buckling constraints of *substructures* (left) and *superstructures* (right) vs. aspect angle  $\beta$  (left) and  $\alpha$  (right) for different complexity  $p$  (left) and  $q$  (right), (steel bars and cables,  $F = 1 \text{ N}$ ,  $L = 1 \text{ m}$ ).

The plot of (58) in Fig. 7 vs.  $\beta$  for different  $p$  shows that (58) has a minimum value at  $p = 2$ . However, the mass at  $p = 2$ , (57), is larger than the mass (43) at  $p = 1$  from Corollary 4.5.

$$f_2 = \frac{t_2}{2 \sin\left(\frac{\alpha}{q-1}\right)}, \quad f_1 = f_2 \cos\left(\frac{\alpha}{q-1}\right). \quad (62)$$

### 5.2. Superstructure bridge with complexity $(n, p, q) = (1, 0, q > 1)$

Refer to Fig. 8 for the notation. The angle between the bars is:

$$\gamma = \frac{2\alpha}{q-1}. \quad (59)$$

The lengths of the bars and cables are:

$$s_0 = \frac{L}{2}, \quad s_1 = s_2 = \frac{L}{2} \sin \alpha, \quad (60)$$

$$b_1 = \frac{L}{2} \cos \alpha, \quad b_2 = L \sin \alpha \sin\left(\frac{\alpha}{q-1}\right).$$

From the equilibrium equations, we obtain the following relations for the forces:

$$t_2 = \frac{F}{2 \left[ \cos \alpha + \sin\left(\frac{\alpha(q-2)}{q-1}\right) / \sin\left(\frac{\alpha}{q-1}\right) \right]}, \quad t_1 = \frac{t_2}{2}, \quad (61)$$

**Theorem 5.3** Consider a superstructure bridge, of total span  $L$ , topology defined by (60), with complexity  $(n = 1, q > 1)$ , Fig. 8. At the yielding condition under a vertical load  $F$  the dimensionless total mass is:

$$\mu_y(\alpha, q) = \frac{t_0}{F} + \frac{(q-1) \sin \alpha}{4 \left[ \cos \alpha + \sin\left(\frac{\alpha(q-2)}{q-1}\right) / \sin\left(\frac{\alpha}{q-1}\right) \right]} + \frac{\rho}{4} \frac{(q-1) \sin \alpha \sin\left(\frac{\alpha}{q-1}\right) + \cos \alpha \cos\left(\frac{\alpha}{q-1}\right)}{\sin\left(\frac{\alpha}{q-1}\right) \cos \alpha + \sin\left(\frac{\alpha(q-2)}{q-1}\right)}. \quad (63)$$

Refer to [30] for an extended proof of the above theorem and following theorems of this section.

**Corollary 5.3** The minimal mass in (63) is achieved at infinite complexity  $q \rightarrow \infty$  and  $t_0 = 0$ . Then the minimal mass at yielding for a superstructure bridge is:

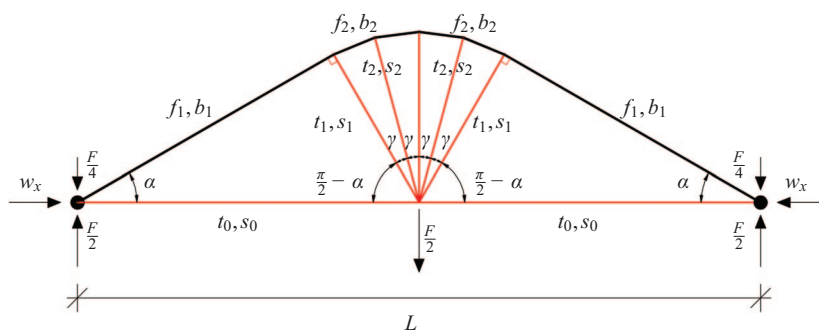


Figure 8. Notations for forces and lengths of bars and cables for a *superstructure* with complexity  $n = 1$  and  $q > 1$ .

$$\mu_Y^*(\alpha_Y^*, q^*) = \frac{1}{4} \left[ (1 + \rho) \arctan \sqrt{\rho} + \sqrt{\rho} \right], \quad (64)$$

where  $q^* \rightarrow \infty$  and the optimal angle  $\alpha_Y^*$  is:

$$\alpha_Y^* = \arctan \sqrt{\rho}. \quad (65)$$

The left side of Fig. 9 illustrates *superstructure* bridges as  $q \rightarrow \infty$ , where masses are given for any  $q$  by (63).

**Proof 5.3** Substitute  $q \rightarrow \infty$  into Eq. (63) to obtain:

$$\mu_Y^*(\alpha, q^* \rightarrow \infty) = \frac{\alpha}{4} (1 + \rho) + \frac{\rho}{4 \tan \alpha}. \quad (66)$$

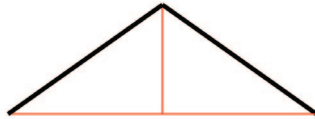
The value of  $a$  that minimizes (66) is (65). See Fig. 6 to see how mass (63) varies with  $q$  and  $a$ . The

optimal  $q^*$  is deduced from the plot of Fig. 6 and the optimal angle is computed analytically in Eq. (65).

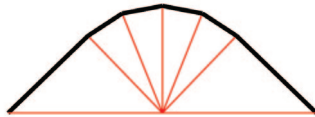
**Theorem 5.4** Consider a superstructure bridge with topology (60), and complexity  $(n, p, q) = (1, 0, q > 1)$ , see Fig. 8. At the buckling condition the dimensionless total mass is:

$$\begin{aligned} \mu_B(\alpha, q) = & \frac{t_0}{F} + \frac{(q-1) \sin \alpha}{4 \left[ \cos \alpha + \sin \left( \frac{\alpha(q-2)}{q-1} \right) / \sin \left( \frac{\alpha}{q-1} \right) \right]} + \\ & \eta \left[ \frac{\cos^2 \alpha \sqrt{\cos \left( \frac{\alpha}{q-1} \right) + 2(q-1) \sin^2 \alpha \sin^2 \left( \frac{\alpha}{q-1} \right)}}{2 \sqrt{\sin \left( \frac{\alpha}{p-1} \right) \cos \alpha + \sin \left( \frac{\alpha(q-2)}{q-1} \right)}} \right]. \end{aligned} \quad (67)$$

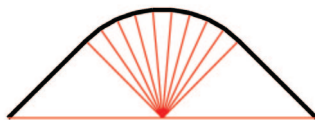
$q = 1, \alpha_Y^* = 35.26 \text{ deg}; \mu_Y^* = 0.7071$



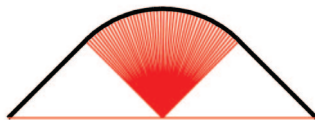
$q = 5, \alpha_Y^* = 43.96 \text{ deg}; \mu_Y^* = 0.6476$



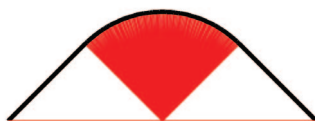
$q = 10, \alpha_Y^* = 44.78 \text{ deg}; \mu_Y^* = 0.6437$



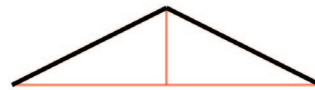
$q = 50, \alpha_Y^* = 44.97 \text{ deg}; \mu_Y^* = 0.6428$



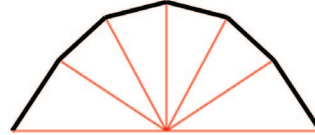
$q = 100, \alpha_Y^* = 44.99 \text{ deg}; \mu_Y^* = 0.6427$



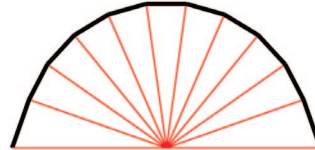
$q = 1, \alpha_B^* = 26.56 \text{ deg}; \mu_B^* = 801.7357$



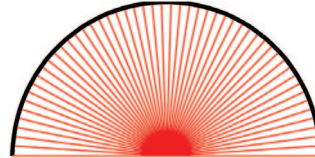
$q = 5, \alpha_B^* = 56.64 \text{ deg}; \mu_B^* = 301.3080$



$q = 10, \alpha_B^* = 70.63 \text{ deg}; \mu_B^* = 181.3748$



$q = 50, \alpha_B^* = 86.21 \text{ deg}; \mu_B^* = 41.7482$



$q = 100, \alpha_B^* = 88.14 \text{ deg}; \mu_B^* = 21.3224$

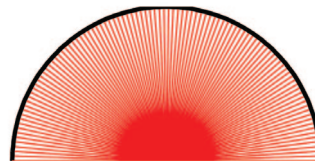


Figure 9. Optimal topologies of *superstructure* bridges with complexity  $(n, p, q) = (1, 0, q \rightarrow \infty)$  under yielding constraints (left) and buckling constraints (right) for different  $q$ , (steel for bars and cables,  $F = 1 \text{ N}, L = 1 \text{ m}$ ).

**Corollary 5.4** *The minimal mass superstructure is achieved for  $q \rightarrow \infty$  and  $t_0 = 0$ , leading to the following mass:*

$$\mu_B(\alpha, q \rightarrow \infty) = \frac{\alpha}{4} + \frac{\eta \cos^2 \alpha}{2\sqrt{\sin \alpha}}. \quad (68)$$

**Proof 5.4** *The plot in Fig. 7 vs.  $\alpha$  for different  $q$  shows that (67) has a global minimum value at  $q \rightarrow \infty$*

It is important to consider that, for the solution  $q \rightarrow \infty$  buckling is not the mode of failure since the lengths of the bars approaches zero. Also note that at  $\alpha = 90$  deg,  $\mu_B = \pi/8$ .

The left side of Fig. 9 shows a sequence of *superstructures* under yielding constraints, as  $q$  increases. From (63) the mass is minimized at  $q \rightarrow \infty$  and  $\alpha_Y^* = 45$  deg ( $\rho = 1$ ). The right side of Fig. 9 shows a sequence of *superstructures* under buckling constraints, as  $q$  increases. From plot in Fig. 7 the mass is minimized at  $\alpha = 90$  deg for  $q = \infty$  ( $\eta = 857.71$ , same steel/steel material as above).

Moreover, the left side of Fig. 10 shows a sequence of *substructures* under yielding constraints, as  $p$  increases. From (53) the mass is minimized at  $p \rightarrow \infty$  and  $\beta_Y^* = 45$  deg ( $\rho = 1$ ). The right side of Fig. 10 shows a sequence of *substructures* under buckling constraints, as  $p$  increases. From plot in Fig. 7 the mass is minimized at  $\beta = 90$  deg for  $p = 1$  ( $\eta = 857.71$ , same steel/steel material as above).

**Theorem 5.5** *A minimal mass superstructure constrained against yielding with hinge/roller boundary conditions, has the same optimal topology as a minimal mass superstructure constrained against buckling and hinge/hinge boundary conditions.*

**Proof 5.5** [31] *proved that the minimal mass structure constrained against yielding with hinge/roller boundary conditions has the topology of the right side of Fig. 9 as  $q \rightarrow \infty$  and  $\alpha \rightarrow 90$  deg. Theorem 5.4 provides the same topology for hinge/hinge constraints.*

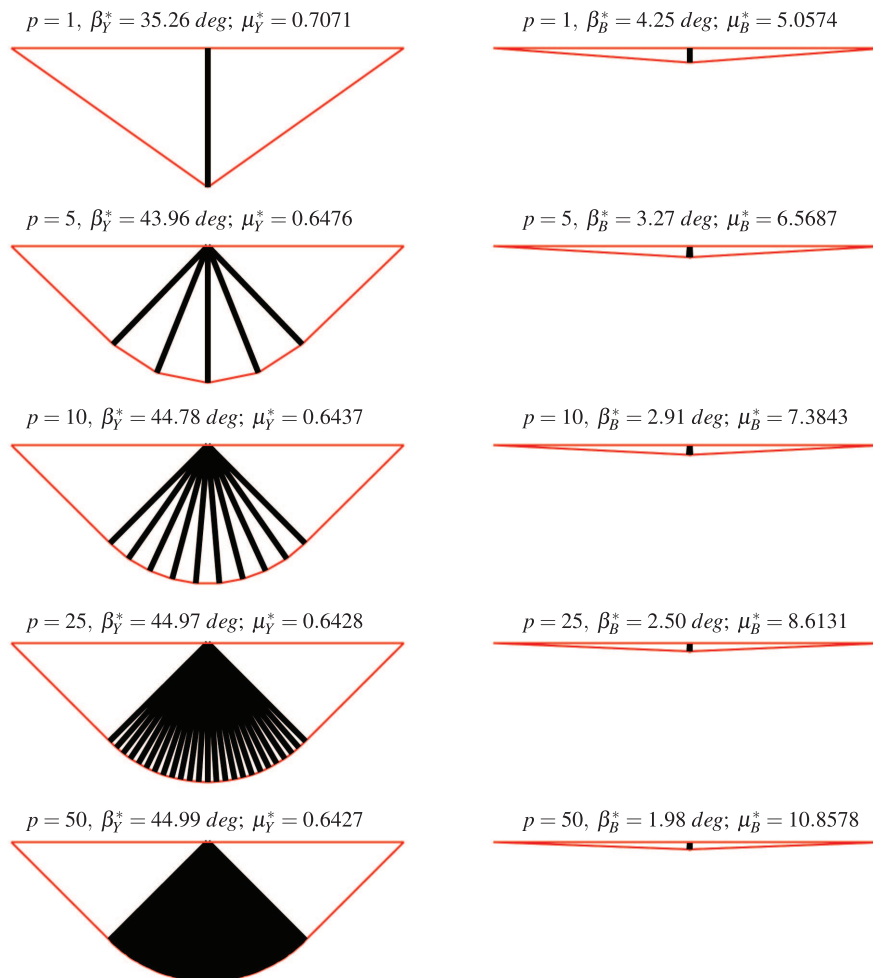


Figure 10. Optimal topologies of *substructure* bridges with  $n = 1$  under yielding constraints (left) and buckling constraints (right) for different  $p$ , (steel for bars and cables,  $F = 1$  N,  $L = 1$  m).

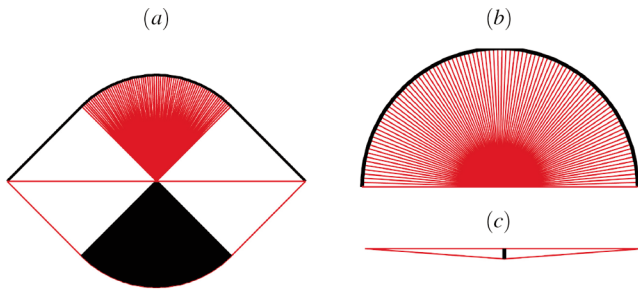


Figure 11. Minimal mass bridges under (a) yielding constrained *nominal* bridges, (b) buckling constrained *superstructure* bridge and (c) buckling constrained *substructure* bridge.

**Theorem 5.6** *The minimal mass nominal bridge constrained against yielding is obtained combining the optimal superstructure topology (Fig. 9, left side as  $q \rightarrow \infty$ ) with the optimal substructure topology (Fig. 9, left side as  $p \rightarrow \infty$ ).*

**Proof 5.6** [31] *obtained these same results by starting with a continuum and optimizing the shape.*

Figure 11(a) illustrates the minimal mass *nominal* bridge under yielding constraints (Theorem 5.6), leading to complexity  $(n, p, q) = (1, \infty, \infty)$ . Fig. 11 (b) illustrates the minimal mass *superstructure* bridge under buckling constraints, leading to complexity  $(n, p, q) = (1, 0, q \rightarrow \infty)$ . Fig. 11(c) illustrates the minimal mass *substructure* bridge under buckling constraints, leading to complexity  $(n, p, q) = (1, 1, 0)$ .

## 6. INTRODUCING DECK AND JOINT MASSES

In previous sections, complexity  $n$  was restricted to 1. This is appropriate only when the external loads are all

applied at the midspan. Real bridges cannot tolerate such an assumption. So in this section we consider a distributed load. Part of the load is the mass of the deck that must span the distance between adjacent support structures (complexity  $n$  will add  $2^n - 1$  supports). In the section 6.4 we will consider adding mass to make the joints, where high precision joints have less mass than rudely constructed joints.

### 6.1. Including deck mass

The total load that the structure must support includes the mass of the deck, which increases with the distance that must be spanned between support points of the structure design (which is determined by the choice of complexity  $n$ ). We therefore consider bridges with increasing complexity  $n$ . We will show that the smallest  $n = 1$  yields smallest structural mass and the largest deck mass. The required deck mass obviously approaches zero as the required deck span approaches zero, which occurs as  $n \rightarrow \infty$ . We will show that the mass of the deck plus the mass of the structure is minimized at a finite value of  $n$ .

The deck, as illustrated in Fig. 12, is composed by  $2^n$  simply supported beams connecting the nodes on the deck. Let the deck parameters be labeled as: mass  $m_d$ , mass density  $\rho_d$ , yielding strength  $\sigma_d$ , width  $w_d$ , thickness  $t_d$  and length equal to:

$$\ell_d = \frac{L}{2^n}. \quad (69)$$

The cross sectional of the deck beam has a moment of inertia equal to:  $I_d = w_d t_d^3 / 12$ . Each beam is assumed to be loaded by a uniformly distributed vertical load

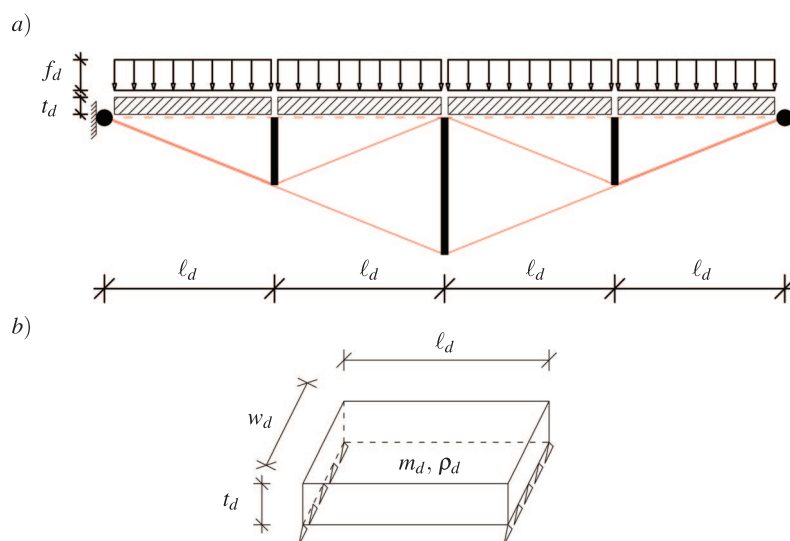


Figure 12. a) schematic deck system for a *substructure* with complexity  $n = 3$  and  $p = 1$ ; b) detail of a single deck module.

summing to the total value  $F$  and the total self weight of the deck ( $\mathcal{F}$ ) ( $g = 9.81ms^{-2}$ ):

$$f_d = \frac{F}{L} + \frac{\mathcal{F}}{L} = \frac{F}{L} + \frac{m_d g 2^n}{L}. \quad (70)$$

Assuming that the beam of a single deck section is simply supported between two consecutive nodes of the bridge, the maximum bending moment is equal to  $fd\ell_d^2/8$  and the maximum stress is given by Navier's equation [32]:

$$\sigma_d = \frac{3 f_d \ell_d^2}{4 w_d t_d^2}. \quad (71)$$

The thickness of the deck beam is:

$$t_d = \frac{m_d}{\rho_d w_d \ell_d}. \quad (72)$$

Substituting (69), (70) and (72) into (71) we get the following equation for the mass of one deck section:

$$m_d = \frac{c_1}{2^{3n}} + \frac{c_1}{2^{2n}} \sqrt{c_2 + \frac{1}{2^{2n}}}, \quad (73)$$

where:

$$c_1 = \frac{3w_d g \rho_d^2 L^3}{8\sigma_d}, \quad c_2 = \frac{16\sigma_d F}{3w_d g^2 L^3 \rho_d^2}. \quad (74)$$

Then, the normalized total mass of the deck structure is:

$$\mu_d^* = \frac{2^n m d}{(\rho_s / \sigma) F L}. \quad (75)$$

The total force acting on each internal node on the deck is then the sum of the force due to the external loads and the force due to the deck:

$$F_{tot} = F + 2^n m d g. \quad (76)$$

### 6.2. Adding deck mass for a substructure bridge with complexity $(n, p, q) = (n, 1, 0)$

In this case, we make use of the notation illustrated in Fig. 13 in which complexity  $p$  is fixed to be one. Complexity  $n$  is defined to be the number of self-similar iterations of the basic module of Fig. 1c. Each iteration  $n = 1, 2, \dots$  generates different lengths of bars and cables. The lengths at the  $i^{th}$  iteration are:

$$b_i = \frac{L}{2^i} \tan \beta, \quad i = 1 - n, \quad (77)$$

$$s_i = \frac{L}{2^i \cos \beta}, \quad i = 1 - n. \quad (78)$$

Observing the multiscale structure of Fig. 13 it's clear that the number of bars and the number of cables at the  $i^{th}$  self-similar iteration are

$$n_{si} = 2^i, \quad n_{bi} = 2^{i-1}. \quad (79)$$

In this case the total force applied to the bridge structure is given by (76) and then the forces in each member become:

$$f_{bi} = \frac{F + 2^n m_{dg}}{2^i}, \quad t_{si} = \frac{F + 2^n m_{dg}}{2^{(1+i)} \sin \beta}. \quad (80)$$

**Theorem 6.1** Consider a substructure bridge with deck mass  $m_d$  and topology defined by (10), (11), (77) and (78), with complexity  $(n, p, q) = (n, 1, 0)$ , see Fig. 13. The minimal mass design under yielding constraints is given by:

$$\mu_Y^* = \left(1 - \frac{1}{2^n}\right) \left(1 + 2^n g \frac{m_d}{F}\right) \sqrt{1 + \rho}, \quad (81)$$

using the optimal angle:

$$\beta_Y^* = \arctan\left(\frac{1}{\sqrt{1 + \rho}}\right). \quad (82)$$

**Proof 6.1** Assuming (77) and (78) for the length of each member, (80) for the forces of each member, and (79) for the number of members, the dimensionless minimal mass becomes:

$$\mu_Y = \frac{1}{2} \left(1 + 2^n g \frac{m d}{F}\right) \left[ \frac{1}{\sin \beta \cos \beta} + \rho \tan \beta \right] \left[ \sum_{i=1}^n \frac{1}{2^i} \right]. \quad (83)$$

yielding,

$$\mu_Y = \frac{1}{2} \left(1 - \frac{1}{2^n}\right) \left(1 + 2^n g \frac{m_d}{F}\right) \left[ \frac{(1 + \tan^2 \beta)}{\tan \beta} + \rho \tan \beta \right]. \quad (84)$$

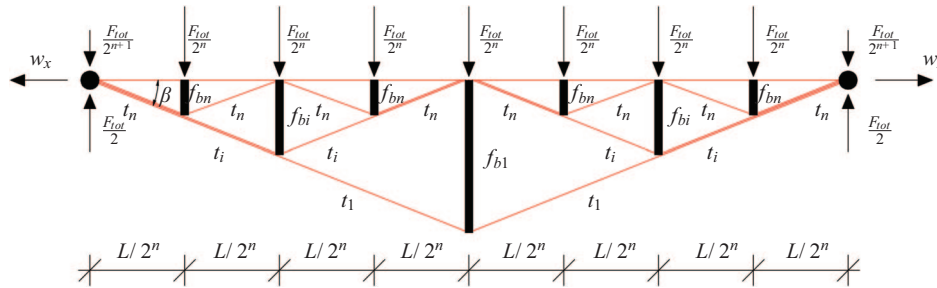


Figure 13. Adopted notations for forces and lengths of bars and cables for a *substructure* with generic complexity  $(n, p, q) = (n, 1, 0)$ .

The solution for minimal mass can be achieved from, where:

$$\frac{\partial \mu_y}{\partial \tan \beta} = \frac{1}{2} \left( 1 - \frac{1}{2^n} \right) \left( 1 + 2^n g \frac{m_d}{F} \right) \left[ -\frac{(\tan^2 \beta + 1)}{\tan^2 \beta} + 2 + \rho \right] = 0, \tag{85}$$

$$\beta_1 = \left( 1 - \frac{1}{2^n} \right) \left( 1 + 2^n g \frac{m_d}{F} \right), \tag{88}$$

$$\beta_2 = \left( \frac{1 + 2\sqrt{2}}{7} \right) \left( 1 - \frac{1}{2^{3n/2}} \right) \sqrt{1 + 2^n g \frac{m_d}{F}}, \tag{89}$$

yielding the optimal angle of (82). Substituting it into (83) concludes the proof.

Observe that (81) yields mass  $\sqrt{1+\rho}/2$  for complexity  $n = 1$  and mass  $\sqrt{1+\rho}$  for complexity  $n = \infty$ . Note from (82), which is the same as (33), that the optimal angle  $\beta_y^*$  does not depend upon the choice of  $n$ . Indeed, the minimal mass solution under yielding constraints (81) depends on the material choice  $\rho$  (14), the complexity parameter  $n$  and the deck properties. Note that, since the total external force  $F$  is a specified constant, the mass is minimized by the complexity  $n = 1$  if  $m_d = 0$ . However since  $m_d$  depends upon  $n$ , the total vertical force including deck mass depends upon  $n$ , and the optimal complexity will be shown to be  $n > 1$  in that case.

**Theorem 6.2** Consider a substructure bridge with topology defined by (10), (11), (77) and (78), with complexity  $(n, p, q) = (n, 1, 0)$ . The minimal mass design under yielding and buckling constraints is given by:

$$\mu_B^* = \beta_1 \frac{(1 + \tan^2 \beta_B^*)}{2 \tan \beta_B^*} + \eta \beta_2 \tan^2 \beta_B^*, \tag{86}$$

using the aspect angle:

$$\beta_B^* = \arctan \left\{ \frac{1}{12\beta_2\eta} \left[ \beta_3 + \beta_1 \left( \frac{\beta_1}{\beta_3} - 1 \right) \right] \right\}, \tag{87}$$

$$\beta_3 = \left( 216\beta_1\beta_2^2\eta^2 - \beta_1^3 + 12\sqrt{324\beta_2^4\eta^4 - 3\beta_1^4\beta_2^2\eta^2} \right)^{1/3}. \tag{90}$$

**Proof 6.2** The total mass of the cables, using (78), (80) and (79), is given by:

$$\mu_s = \left( \frac{1 + \tan^2 \beta}{2 \tan \beta} \right) \left( 1 - \frac{1}{2^n} \right) \left( 1 + 2^n g \frac{m_d}{F} \right). \tag{91}$$

Similarly, making use of (4), the total mass of bars is:

$$\mu_b = \eta \tan^2 \beta \left( \frac{1 + 2\sqrt{2}}{7} \right) \left( 1 - \frac{1}{2^{3n/2}} \right) \sqrt{1 + 2^n g \frac{m_d}{F}}. \tag{92}$$

Introducing constants  $\beta_1$  and  $\beta_2$  given in (88) and (89), the total mass is:

$$\mu_B = \mu_s + \mu_b = \beta_1 \frac{(1 + \tan^2 \beta)}{2 \tan \beta} + \eta \beta_2 \tan^2 \beta. \tag{93}$$

The solution for minimal mass can be achieved from,

$$\frac{\partial \mu_B}{\partial \tan \beta} = \beta_1 \left( 1 - \frac{1 - \tan^2 \beta}{2 \tan^2 \beta} \right) + 2\eta \beta_2 \tan \beta = 0, \tag{94}$$

yielding the optimal angle of (87) by solving the following cubic equation:

$$4 \frac{\beta_2}{\beta_1} \eta \tan^3 \beta + \tan^2 \beta - 1 = 0. \quad (95)$$

$$\mu_Y^* = \left(1 - \frac{1}{2^n}\right) \left(1 + 2^n g \frac{m_d}{F}\right) \sqrt{\rho(1+\rho)}, \quad (99)$$

Substituting (87) into (93) concludes the proof.

using the aspect angle:

### 6.3. Adding deck mass for a superstructure bridge with complexity $(n, p, q) = (n, 0, 1)$

$$\alpha_Y^* = \arctan\left(\sqrt{\frac{\rho}{1+\rho}}\right). \quad (100)$$

In this case, we make use of the notation illustrated in Fig. 14 in which complexity  $q$  is fixed to be one. Complexity  $n$  is the number of self-similar iterations of the basic module of Fig. 1b at different scales. After the  $i^{th}$  self-similar iterations, the length of the bars and cables for  $i$  ranging from 1 to  $n$ , are:

**Theorem 6.4** Consider a superstructure bridge with topology defined by (10), (12), (96), and complexity  $(n, p, q) = (n, 0, 1)$ , see Fig. 14. The structure is loaded with a given total vertical force (76) and the minimal bar mass, subject to yielding constraints is given by:

$$b_i = \frac{L}{2^i \cos \alpha}, \quad s_i = \frac{L}{2^i} \tan \alpha. \quad (96)$$

$$\mu_B^* = \frac{\delta_1}{2} + \eta \delta_2 \frac{5^{5/4}}{4}, \quad (101)$$

Observing the multiscale structure of Fig. 14 it's clear that the number of bars and the number of cables after the  $i^{th}$  self-similar iterations are:

using the aspect angle:

$$\alpha_B^* = \arctan \frac{1}{2}, \quad (102)$$

$$n_{si} = 2^{i-1}, \quad n_{bi} = 2^i. \quad (97)$$

where:

In this case the total force applied to the bridge structure is given by (76) and then the forces in each member become:

$$\delta_1 = \frac{1}{2} \left(1 + 2^n g \frac{m_d}{F}\right) \left(1 - \frac{1}{2^n}\right), \quad (103)$$

$$f_{bi} = \frac{F + 2^n m_d g}{2^{(i+1)} \sin \alpha}, \quad t_{si} = \frac{F + 2^n m_d g}{2^i}. \quad (98)$$

$$\delta_2 = \sqrt{2} \left(\frac{1 + 2\sqrt{2}}{7}\right) \sqrt{1 + 2^n g \frac{m_d}{F}} \left(1 - \frac{1}{2^{3n/2}}\right). \quad (104)$$

**Theorem 6.3** Consider a superstructure bridge with topology defined by (10), (12), (96), with complexity  $(n, p, q) = (n, 0, 1)$ , Fig. 14. Under a given total vertical force (76), the minimal mass design under yielding constraints is given by:

The proofs of Theorems 6.3 and 6.4 can be found in [30]. Figures 15 and 16 show the optimal masses for yielding and buckling with and without deck mass. The optimal substructures and superstructures are presented in Figs. 17 and 18 respectively. The addition of deck mass causes, in all considered cases, an optimal complexity  $n$  that tends to infinity. In the next section we will consider the addition of joint mass.

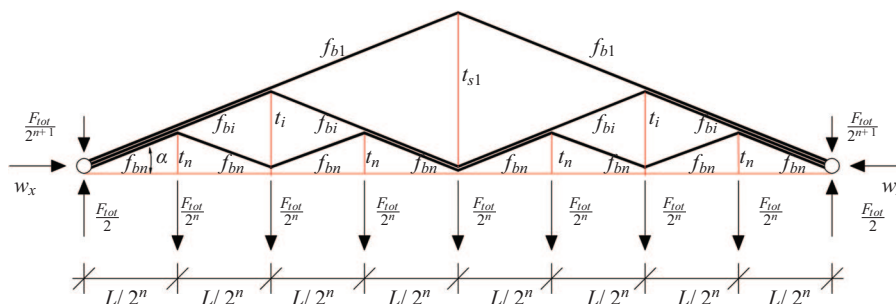


Figure 14. Adopted notations for forces and lengths of bars and cables for a superstructure with complexity  $(n, p, q) = (n, 0, 1)$ .

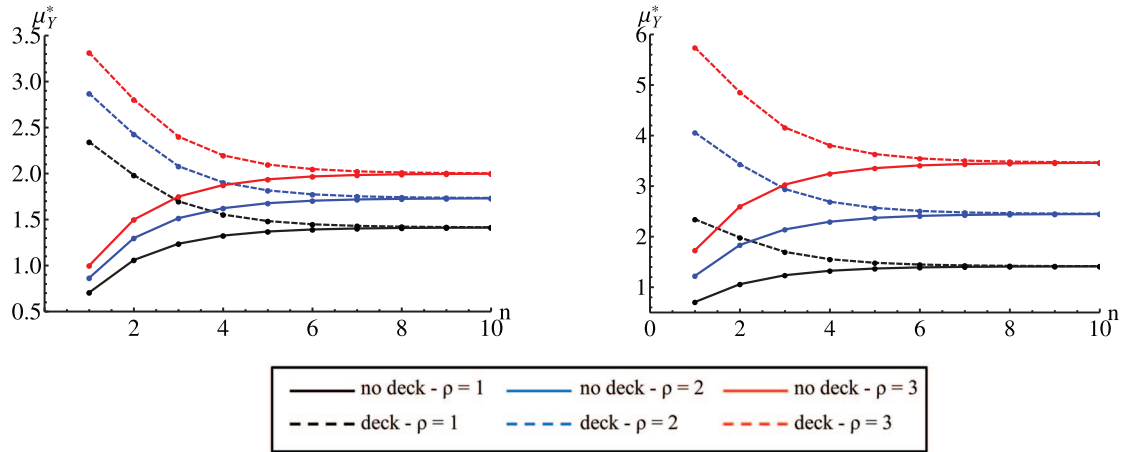


Figure 15. Optimal masses under yielding of the *substructures* (left) and *superstructure* (right) without deck (solid curves) and with deck (dashed curves) for different values of the complexity  $n$  and for different values of  $\rho$ , ( $F = 1 N$ ,  $L = w_d = 1 m$ , steel deck).

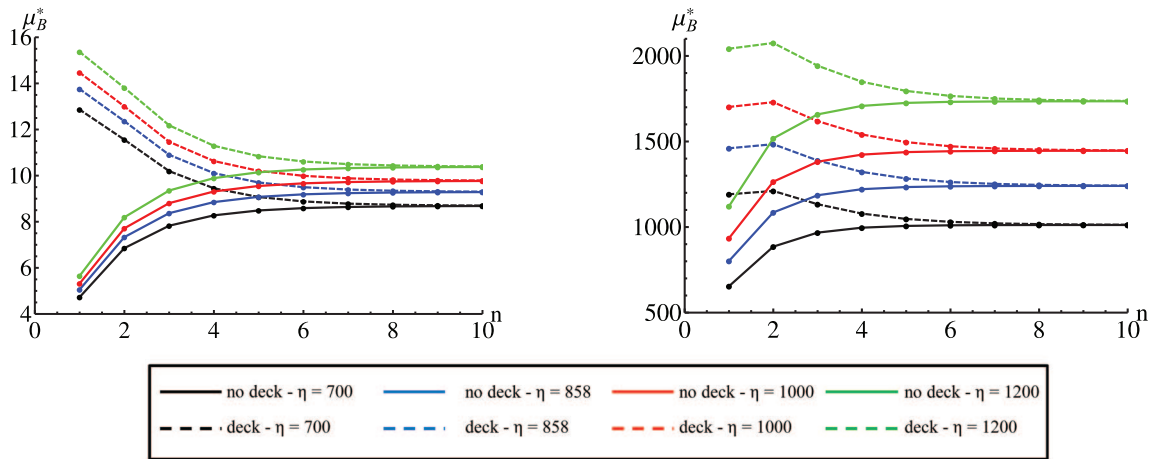


Figure 16. Optimal masses under buckling of the *substructures* (left) and *superstructure* (right) without deck (solid curves) and with deck (dashed curves) for different values of the complexity  $n$  and for different values of  $\eta$ , ( $F = 1 N$ ,  $L = w_d = 1 m$ , steel deck).

### 6.4. Penalizing complexity with cost considerations: adding joint mass

Theorem 6.1, for  $m_d = 0$ , leads to an optimal complexity  $n = 1$  which corresponds to a minimal mass equal  $\sqrt{1+\rho}/2$ . As complexity  $n$  approaches infinity, instead, the mass given in (81), for  $m_d = 0$ , go to a limit equal to  $\sqrt{1+\rho}$ . However, the addition of the deck mass in Theorem 6.1 switches the optimal complexity from  $n = 1$  to  $n = \infty$ , so small complexities  $n$  are penalized by massive decks. Also in this latter case, the resulting optimal minimal mass is then  $\sqrt{1+\rho}$ , as can be verified looking the (81) or considering that as  $n$  goes to infinity the deck mass given in (73) approaches zero. As a matter of fact, neither  $n = 1$  or  $n = \infty$  are believable solutions due to practical reasons: the first solution leads only to a single force at the middle of the span, the second

solution leads to an infinite number of joints and connections. The minimal masses obtained from (81) with or without deck correspond to perfect massless joints. The addition of the joint masses to a tensegrity structure with  $n_n$  nodes, as illustrated in [10], leads to the following total normalized mass:

$$\mu_{Y,tot}^* = \mu_Y^* + \mu_d^* + \Omega n_n. \tag{105}$$

Let  $\$_j$  be the cost per *kg* of making joints and let  $\$_b$  be the cost per *kg* of making bars. Then define  $\Omega = \$_j/\$_b$ . For perfect joints  $\Omega = 0$ , for rudely made low cost joints  $\$_j$  is small and  $\Omega$  is larger. Hence  $\Omega$  is also approximatively the ratio of material cost per joint divided by material cost per structural member being joined.

Consider the minimal masses of the *substructure* bridge ( $\mu_Y^*$ ) constrained against yielding, for the cases with or without deck, see Eq. (81). Assume steel material for cables, bars and deck beams and set  $F = 1$

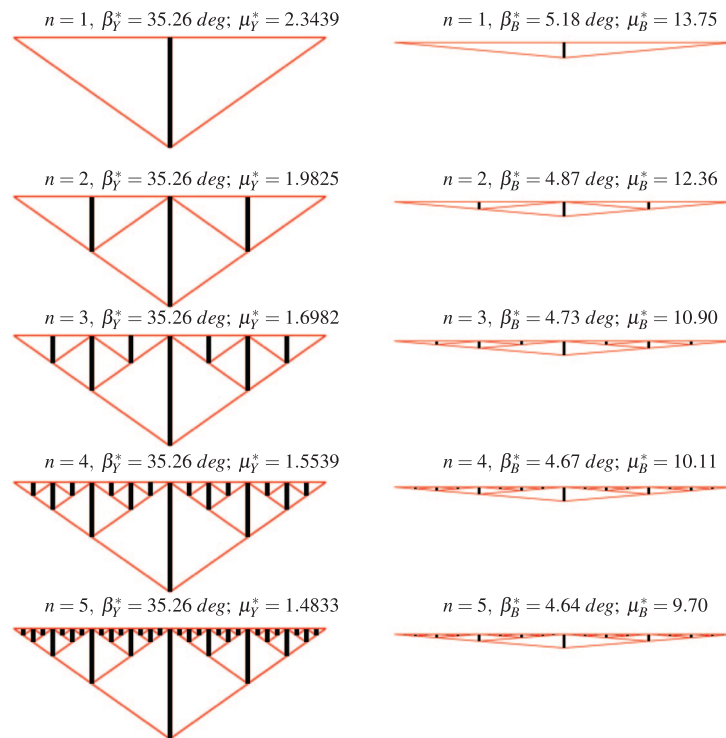


Figure 17. Optimal topologies of *substructure* bridges with complexity  $(n, p, q) = (n \rightarrow \infty, 1, 0)$  under yielding constraints (left) and buckling constraints (right) for different  $n$ , (steel for bars, cables and deck,  $F = 1 N$ ,  $L = W_d = 1 m$ ).

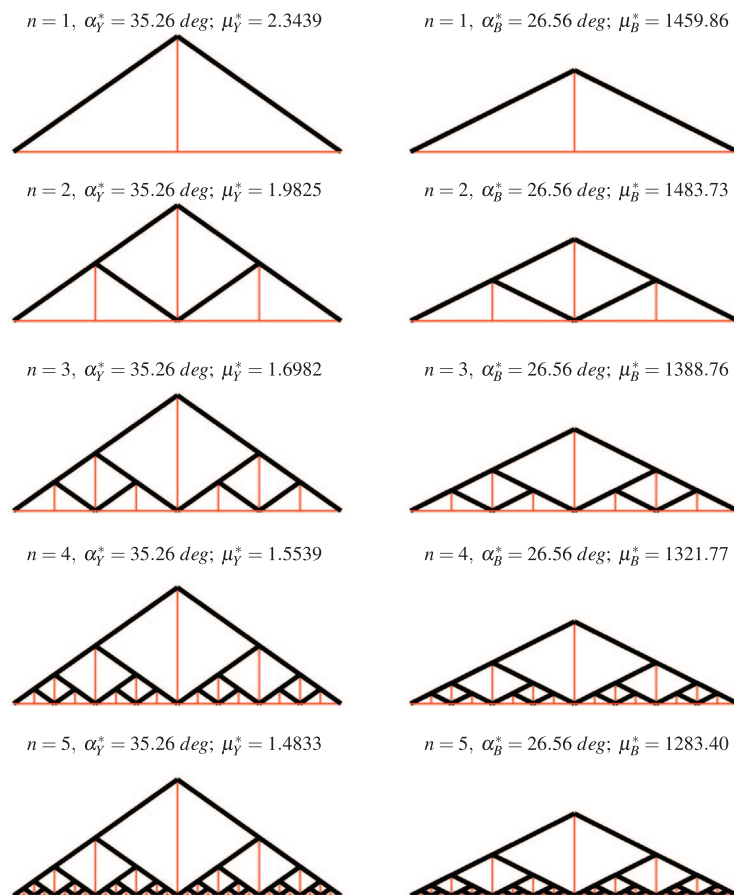


Figure 18. Optimal topologies of *superstructure* bridges with complexity  $(n, p, q) = (n \rightarrow \infty, 0, 1)$  under yielding constraints (left) and buckling constraints (right) for different  $n$ , (steel for bars, cables and deck,  $F = 1 N$ ,  $L = w_d = 1 m$ ).

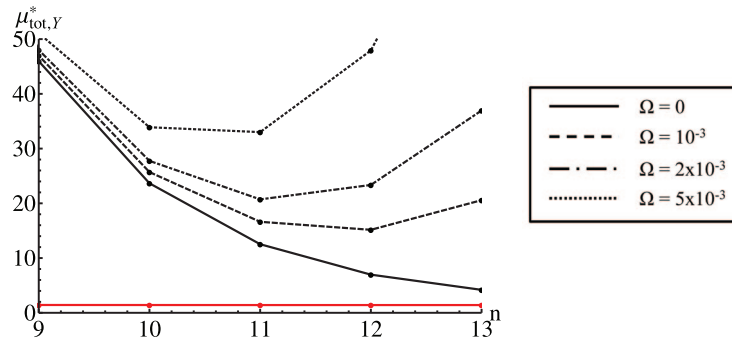


Figure 19. Optimal masses under yielding of the *substructures* and *superstructure* (red curve) and total optimal mass with deck and different joint factors (dashed and dotted curves) for different values of the complexity  $n$  (steel for bars, cables, deck,  $F = 1 N, L = w_d = 1 m$ ).

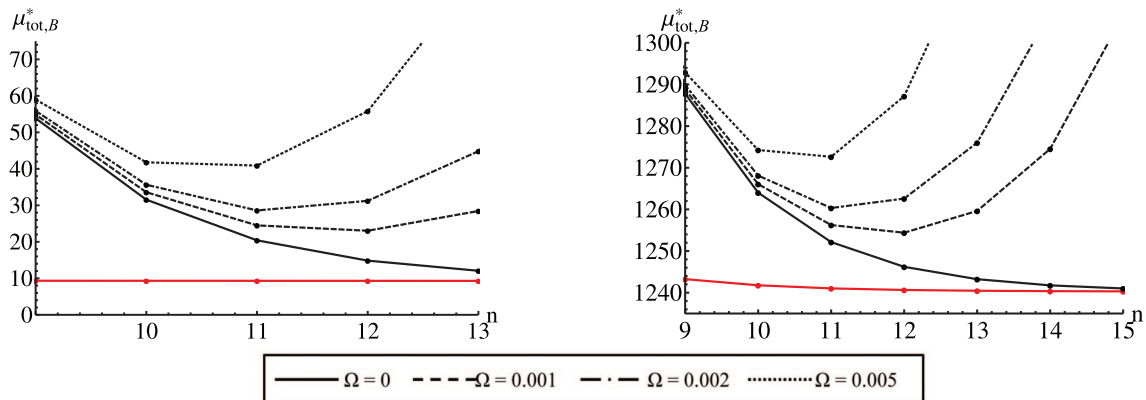


Figure 20. Optimal masses under buckling of the *substructures* (left) and *superstructure* (right) (red curves) and total optimal masses with deck and different joint factors (dashed and dotted curves) for different values of the complexity  $n$  (steel for bars, cables, deck,  $F = 1 N, L = w_d = 1 m$ ).

$N, L = w_d = 1 m$ . Without deck the optimal aspect angle  $\beta_y^*$  (82) is  $35.26 \text{ deg}$ . For the case with neither deck nor joint mass, the optimum complexity  $n$  is 1, which corresponds to an optimal mass  $\mu_y^* = \sqrt{2}/2$ . As  $n$  approaches infinity the mass tends to a limit equal to  $\sqrt{2}$ , which is also the optimal mass for the case with deck mass and perfectly manufactured joints, since  $\mu_d^*$  approaches zero for  $n \rightarrow \infty$ . Note that with the addition of joint masses as illustrated in (105), the optimal complexity  $n^*$  can become a finite value. The above procedure can be also used for the design under buckling constraints.

Figures. 19 (for yielding) and Fig. 20 (for buckling) show the total minimal masses obtained by using (105). In both Figs. 19 and 20 we also show with red curves the minimal mass of *substructures* or *superstructures* only. In either case, the total mass of the structure with deck (but no joint mass), is shown by black continuous lines in Figs. 19 and 20, reaching minimum for an infinite complexity  $n$ . It is worth

noting that, for infinite  $n$ , the mass of the deck is zero and the total minimum mass is just the mass of the bridge structure. Then, with the dotted and dashed lines, we show that a finite optimal complexity can be achieved if the joint's masses are considered.

From Fig. 19 note that the minimal mass ( $\mu \cong 21$ ) bridge has complexity  $n = 11$  for  $\Omega = 0.002$ , and has minimal mass  $\mu \cong 15$  with complexity  $n = 12$  for  $\Omega = 0.001$ . Economic costs would decide if saving 25 % structural mass is worth the extra cost of improving the joint precision by a factor of 2.

## 7. CONCLUDING REMARKS

This paper provides closed form solutions (analytical expressions) for minimal mass tensegrity bridge designs. The forces, locations, and number of members are optimized to minimize mass subject to both buckling and yielding constraints for a planar structure with fixed-hinge/fixed-hinge boundary conditions.

We designed bridges from the elementary consideration of i) yielding constraints, ii) buckling constraints, iii) without deck mass, iv) with deck mass,

v) *superstructure* only, vi) *substructure* only, vii) without joint mass, viii) with joint mass.

We optimize the complexity of the structure, where structural complexity as the number of members in the design. This can be related to 3 parameters  $(n, p, q)$ , where  $2^n$  is the number of deck sections along the span;  $p$  is the number of compressive members (bars) reaching from the span center to the *substructure*; and  $q$  is the number of cables reaching from the span center to the *superstructure*. Hence we refer to  $(n, p, q)$  as the three different kinds of *complexities* of the structure. We used a tensegrity structural paradigm which allowed these several kinds of complexities. The complexity  $n$  is determined by a self-similar law to fill the space of the bridge. As the number of self-similar iterations go to infinity we get a tensegrity fractal topology. However, the number of self-similar iterations  $n$  and the complexities  $p$  and  $q$  required to minimize mass, under different circumstances within the set of 8 possibilities i),...,viii) listed above, go to an optimal number between 1 and infinity, where an infinite complexity fills the define space with a continuum.

First we optimized structures under yielding constraints for the simply-supported case ( $n = 1$ ) with no deck. The number of self-similar iterations  $n$  of the given tensegrity module goes to infinity as the mass approaches the minimum. Our result produces the same topology as [31], where there is a compressive member at  $45 \text{ deg}$  attached at each boundary, connecting to a  $1/4$  pie shaped continuum material piece at the center. The bottom half of the bridge (the *substructure*) is the *dual* of the *superstructure* (*dual* meaning flip the structure about the horizontal axis and replace all tension members with compression members and all tension members with compressive members). We showed that the top half of this structure is the optimal topology for bridge designs which do not allow any *substructure*, and conversely that the bottom half of this structure is the optimal topology for bridges allowing no *superstructure*.

Secondly, we optimized the simply supported bridge ( $n = 1$ ) under buckling constraints with no deck. For the *superstructure* design we proved that the minimal mass is achieved at high values of  $q$ , approaching a continuum (where the shape of the structure is a half disk). It is interesting that this shape (designed under buckling constraints) is the same as the result of [31], which was derived under *yielding* constraints and different boundary conditions (our conditions were hinge/hinge and his were hinge/roller). We also optimized the *substructure*

bridge (without deck) to find an optimal complexity  $(n, p, q) = (1, 1, 0)$ . This *substructure* bridge has less mass than the *superstructure* bridge except for extremely high complexity ( $q > 400$ ). At  $q = 3000$ , the *superstructure* has one fifth the mass of the *substructure* design. Thirdly, we consider adding a deck to the bridge, since this is the only practical possibility to carry distributed loads. Under *yielding* constraints the minimal mass bridge requires infinite complexity  $n$  (infinite self-similar iterations of the tensegrity module). The bridge has *superstructure* and *substructure* that are duals of each other. The angle of departure from the boundaries is  $35.26 \text{ deg}$  (as opposed to  $45 \text{ deg}$  for the no deck mass discussed above). Under buckling constraints the structure  $(n, p, q) = (n, 1, 1)$  has minimal mass at  $n = \infty$ . The *superstructure* has a departure angle (from the boundary) of approximately  $26.56 \text{ deg}$  as opposed to larger angles for yielding designs and no-deck designs. The *substructure* under buckling constraints has an even more streamlined profile with departure angle approximately of  $5.18 \text{ deg}$ . Furthermore the mass of a *substructure* design is much smaller that the mass of a *superstructure* design.

In all of the design cases studied, we conclude that the infinite complexity *substructure* bridge is the solution which minimizes the sum of deck mass and structural mass.

Finally, we consider the impact of assigning a mass penalty to the number of required joints. We suppose that the cost per  $kg$  of compressive members is  $\$b$ , and that the cost per  $kg$  of fabricated joints is  $\$j$ . The ratio  $\Omega = \$b/\$j$  is used as a weighting factor to add joint mass to member mass and this sum is minimized. The total minimal mass is always at a finite complexity  $n < \infty$  and  $p = q = 1$ . Again, buckling is always the mode of failure in our study, leading to the conclusion that with deck mass and joint mass, this paper describes the optimal complexity to obtain a minimal mass bridge, and this bridge is not a continuum (as Michell produced under yielding assumptions), but, has finite complexity  $n$ . The optimal complexity  $n$  is given in terms of fabrication costs and material properties.

The tensegrity architectures introduced in the present work allow for creating networks of tension and compressive members at many different scales [10,28], which simultaneously work as load-carrying members of the structure and as sensing and actuating functions.

This study paves the way for further studies on: stiffness and stability [11]; vibrations modes and

control [33]. It is predictable that the prestrain will play a fundamental rule on the tuning of stiffness and dynamics of such structures. For sake of brevity these issues must appear in future work.

In future work, we plan to employ the present multiscale approach for the optimal design of composite tensegrity structures [34–36]; tensegrity metamaterials featuring special mechanical and directional behaviors [5, 6]; and bio-inspired membrane networks with tensegrity architecture [20, 37, 38].

## REFERENCES

- [1] Fuller, R. B., Tensile-integrity structures. United States Patent 3,063,521, 1962. Filed 31 August 1959, Granted 13 November 1962.
- [2] Lalvani, H. (Editor), Origins of tensegrity: views of Emmerich, Fuller and Snelson, *Int. J. Space Struct.*, 1996, 11(1–2), 27–55.
- [3] Ingber, D. E., The architecture of life, *Scientific American*, 1998, 278, 1, 48–57.
- [4] Snelson, K. D., Continuous tension, discontinuous compression structures. United States Patent 3,169,611, 1965. Filed 14 March 1960, Granted 16 February 1965.
- [5] Fraternali, F., Senatore, L. and Daraio, C., Solitary waves on tensegrity lattices, *J. Mech. Phys. Solids*, 2012, 60, 1137–1144.
- [6] Fraternali, F., Carpentieri, G., Amendola, A., Skelton, R.E. and Nesterenko, V.F., Multiscale tunability of solitary wave dynamics in tensegrity metamaterials, *Appl. Phys. Letters*, 2014, 105, 201903.
- [7] Iori T. and Poretti S., Storia dell'ingegneria strutturale in Italia. Gangemi Editore, Roma, 2014. ISBN: 978-88-492-7830-9.
- [8] Skelton, R.E. and de Oliveira, M.C., Optimal complexity of deployable compressive structures, *J. Franklin I.*, 2010, 347, 228–256.
- [9] Skelton, R.E. and de Oliveira, M.C., Optimal tensegrity structures in bending: the discrete Michell truss, *J. Franklin I.*, 2010, 347, 257–283.
- [10] Skelton, R. E. and de Oliveira, M. C., Tensegrity Systems, Springer, 2010.
- [11] Nagase, K. and Skelton, R. E., Minimal mass tensegrity structures, *Journal of the International Association for Shell and Spatial Structures*, 2014, 55(1), 37–48.
- [12] Koohestani, K., Form-finding of tensegrity structures via genetic algorithm, *Int. J. Solids Struct.*, 2012, 49, 739–747.
- [13] Rhode-Barbarigos, L., Jain, H., Kripakaran, P. and Smith, I.F.C., Design of tensegrity structures using parametric analysis and stochastic search, *Eng. Comput.*, 2010, 26(2), 193–203.
- [14] Sakamoto, T., Ferrè, A. and Kubo, M., (Eds.) From Control to Design: Parametric/Algorithmic Architecture, Actar, 2008.
- [15] Sokóf, T. and Rozvany, G.I.N., New analytical benchmarks for topology optimization and their implications. Part I: bi-symmetric trusses with two point loads between supports, *Struct. Multidisc. Optim.*, 2012, 46, 477–486.
- [16] Tilbert, A. G. and Pellegrino, S., Review of Form-finding methods for tensegrity structures, *Int. J. Space Struct.*, 2011, 18, 209–223.
- [17] Yamamoto, M., Gan, B. S., Fujita, K. and Kurokawa, J., A genetic algorithm based form-finding for tensegrity structure, *Procedia Engineering*, 2011, 14, 2949–2956.
- [18] Fraternali, F., Marino, A., El Sayed, T. and Della Cioppa, A., On the Structural Shape Optimization through Variational Methods and Evolutionary Algorithms, *Mech. Adv. Mater. Struc.*, 2011, 18, 224–243.
- [19] Bel Hadj Ali, N., Rhode-Barbarigos, L., Pascual Albi, A.A. and Smith, I.F.C., Design optimization and dynamic analysis of a tensegrity-based footbridge, *Eng. Struct.*, 2010, 32(11), 3650–3659.
- [20] Fraternali, F., Farina, I. and Carpentieri, G., A discrete-to-continuum approach to the curvatures of membrane networks and parametric surfaces, *Mech. Res. Commun.*, 2014, 56, 18–15.
- [21] Phocas, M. C., Kontovourkis, O. and Matheou, M., Kinetic hybrid structure development and simulation, *Int. J. Archit. Comput.*, 2012, 10(1), 67–86.
- [22] Baker, W. F., Beghini, L. L., Mazurek, A., Carrion, J. and Beghini, A., Maxwell's reciprocal diagrams and discrete Michell frames, *Struct. Multidisc. Optim.*, 2013, Online first, doi: 10.1007/s00158-013-0910-0.
- [23] Fraternali, F., Angelillo, M. and Fortunato, A., A lumped stress method for plane elastic problems and the discrete-continuum approximation, *Int. J. Solids Struct.*, 2002, 39, 6211–6240.
- [24] Fraternali, F., A thrust network approach to the equilibrium problem of unreinforced masonry vaults via polyhedral stress functions, *Mech. Res. Commun.*, 2010, 37, 198–204.
- [25] Fraternali, F., A mixed lumped stress - displacement approach to the elastic problem of masonry walls, *Mech. Res. Commun.*, 2010, 38, 176–180.
- [26] Fraternali, F. and Carpentieri, G., On the correspondence between 2D force networks and polyhedral stress functions, *Int. J. Space Struct.*, 2013, 29(3), 145–159.
- [27] Skelton, R. E. and Nagase, K., Tensile tensegrity structures, *Int. J. Space Struct.*, 2012, 27, 131137.
- [28] Skelton, R. E., Fraternali, F., Carpentieri, G. and Micheletti, A., Minimum mass design of tensegrity bridges with parametric architecture and multiscale complexity, *Mech. Res. Commun.*, 2014, 58, 124–132, ISSN 0093–6413, doi: 10.1016/j.mechrescom.2013.10.017.
- [29] Skelton, R.E., Structural systems: a marriage of structural engineering and system science, *J. Struct. Control*, 2002, 9, 113–133.
- [30] Carpentieri, G., Skelton, R. E. and Fraternali, F., On the Minimum Mass and Optimal Complexity of Planar Tensegrity Bridges, Internal Report of the University of California, San Diego, Mechanical and Aerospace Engineering, No. 1-2014. available at url: [www.fernandofraternaliresearch.com/publications/arxivTensegrity-bridgesJheoryC2014.pdf](http://www.fernandofraternaliresearch.com/publications/arxivTensegrity-bridgesJheoryC2014.pdf) (last accessed: June 23, 2015).
- [31] Michell, A. G. M., The limits of economy of material in frame-structures, *Philos. Mag.*, 1904, 8, 589–597.
- [32] Gere, J. M. and Timoshenko, S. P., Mechanics of Materials, PWS Publishing Company, 1997.

- [33] Nagase, K. and Skelton, R. E., Network and vector forms of tensegrity system dynamics, *Mech. Res. Commun.*, 2014, 59, 14–25.
- [34] Ascione, L. and Fraternali, F., A Penalty Model for the Analysis of Composite Curved Beams, *Comput. & Struct.*, 1992, 45, 985–999.
- [35] Fraternali, F. and Reddy, J. N., A Penalty Model for the Analysis of Laminated Composite Shells, *Int. J. Solids Struct.*, 1993, 30, 3337–3355.
- [36] Fraternali, F. and Bilotti, G., Non-Linear Elastic Stress Analysis in Curved Composite Beams, *Comput. & Struct.*, 1997, 62, 837–869.
- [37] Fraternali, F., Lorenz, C. D. and Marcelli, G., On the estimation of the curvatures and bending rigidity of membrane networks via a local maximum-entropy approach, *J Comput. Phys.*, 2012, 231, 528–540.
- [38] Schmidt, B. and Fraternali, F., Universal formulae for the limiting elastic energy of membrane networks, *J. Mech. Phys. Solids*, 2012, 60, 172–180.

